Vented-Box Loudspeaker Systems Part I: Small-Signal Analysis

RICHARD H. SMALL

School of Electrical Engineering, The University of Sydney, Sydney, N.S.W. 2006, Australia

The low-frequency performance of a vented-box loudspeaker system is directly related to a small number of easily measured system parameters. This system is a fourth-order (24-dB per octave cutoff) high-pass filter which can be adjusted to have a wide variety of response characteristics. Enclosure losses have a significant effect on system performance and should be taken into account when assessing or adjusting vented-box systems. The efficiency of a vented-box loudspeaker system is shown to be quantitatively related to system frequency response, internal losses, and enclosure size.

LIST OF IMPORTANT SYMBOLS

f_B	Resonance frequency of vented enclosure
f_H	Frequency of upper voice-coil impedance peak
f_L	Frequency of lower voice-coil impedance peak
f_M	Frequency of minimum voice-coil impedance between f_L and f_H
f_S	Resonance frequency of driver
f_{SB}	Resonance frequency of driver mounted in enclosure
f_3	Half-power (-3 dB) frequency of loudspeaker system response
$G(s)$	Response function
h	System tuning ratio, $= f_B/f_S$
k_P	Power rating constant
k_η	Efficiency constant
P_{AR}	Displacement-limited acoustic power rating
P_{ER}	Displacement-limited electrical power rating
$P_{E(\max)}$	Thermally limited maximum input power
Q_A	Enclosure Q at f_B resulting from absorption losses
Q_B	Total enclosure Q at f_B resulting from all enclosure and vent losses
Q_L	Enclosure Q at f_B resulting from leakage losses
Q_P	Enclosure Q at f_B resulting from vent frictional losses
Q_{ES}	Driver Q at f_S considering electrical resistance R_E only
Q_{MS}	Driver Q at f_S considering driver nonelectrical losses only
Q_{TS}	Total driver Q at f_S resulting from all driver resistances
Q_T	Total driver Q at f_S resulting from all system resistances
R_E	Dc resistance of driver voice coil
V_{AS}	Volume of air having same acoustic compliance as driver suspension
V_B	Net internal volume of enclosure
V_D	Peak displacement volume of driver diaphragm
$x_{\max}$	Peak linear displacement of driver diaphragm
$X(s)$	Displacement function
α	System compliance ratio, $= V_{AS}/V_B$
η_0	Reference efficiency.

1. INTRODUCTION

Historical Background

The concept of the vented loudspeaker enclosure was introduced by Thuras in a U.S. patent application of 1930 [1]. The principle of operation of the system is described in considerable detail in this document which recognizes the interaction of diaphragm and vent radiation, presents several possible methods of construction, and includes a polynomial expression for the frequency-dependent behavior.

In 1952 Locanthi [2] provided the first means of calculating the exact magnitude of diaphragm–vent interaction and introduced the use of electrical analog networks to study the performance of vented-box systems.

In 1954 Beranek [3, ch. 8] derived a polynomial expression for the response of a vented-box system which was much simpler than Thuras' expression. Beranek ignored diaphragm–vent interaction and gave results for the relative response at three discrete frequencies, taking into account the system losses and including the exact effects of the variation with frequency of the radiation load resistance.

The first successful attempt to penetrate both the analysis and design of the vented-box system was published by van Leeuwen in 1956 [4]. This paper examines diaphragm–vent interaction and the effects of both parallel and series resistance in the vent. The analysis gives polynomial expressions for the frequency response and indicates the system poles and their relationship to the system transient response. Van Leeuwen studied the voice-coil impedance and determined accurate methods of calculating the driver and system parameters (and their nonlinearities) from measurement of this impedance. Also, he presented system design methods for obtaining a response characteristic of the equal-ripple (Chebyshev) type and illustrated the use of analog circuits to study the voice-coil impedance and the steady-state and transient response of the system. Unfortunately, this paper was published only in Dutch and was not widely read.

In 1959 de Boer [5], incorporating the diaphragm–vent interaction analysis of Lyon [6], showed clearly that the problem of vented-box system design was a problem of high-pass filter synthesis. Working independently, Novak [7] published in the same year an analysis which provided a simplified transfer function, methods for determining the driver and system parameters from voice-coil impedance measurements, and a clear indication of the amount of driver damping required for flat response.

A year later, Keibs [8] published a penetrating analysis which provided specific quantitative design criteria for the conditions of maximally flat amplitude response and optimum (as defined) transient response.

In 1961 two papers published almost simultaneously but independently brought the understanding of vented-box systems in English-language publications up to and beyond the level attained by van Leeuwen. First de Boer, who had in fact read van Leeuwen's paper, extended his own earlier approach using network-synthesis techniques to provide a much more lucid result. De Boer's paper [9] provides design solutions for both Butterworth and Chebyshev responses. While de Boer's analytical approach can only be described as elegant, the paper is mainly theoretical and does not provide any detailed guide to physical realization.

Later in 1961, Thiele [10], working with the simplified model established by Novak [7], published an analysis which included exhaustive treatment of the practical matters of realization. It is interesting that Thiele's paper, written completely independently of de Boer's, follows almost exactly the analysis–approximation–synthesis procedure outlined by de Boer in his introduction. Thiele's paper provides a much wider range of "optimum" responses than any previous paper, treats the amplifier as an integral part of the system, and provides simple and accurate methods of determining both driver and system parameters through measurement of the voice-coil impedance. It is probably fair to say that Thiele's paper was the first to provide an essentially complete, comprehensive, and practical understanding of vented-box systems on a quantitative level.

While both de Boer and Thiele published in English, neither paper appears to have been widely read (or understood) at the time of publication. Only after 10 years has Thiele's paper been recognized as a classic and republished for a wider audience.

In 1969 Nomura [11] pointed out that enclosure losses often contribute substantial response errors. Nomura's paper provides design solutions for Chebyshev, "degenerated" Chebyshev, and Butterworth responses which include the effects of absorption losses in the enclosure.

A very recent paper by Benson [32] contains the most complete small-signal treatment of vented-box systems yet available and covers several interesting topics not discussed here. A number of footnotes have been added to the text of this paper to make reference to the improved understanding or techniques developed by Benson or to indicate areas in which further information may be gained from his paper.

Technical Background

The vented-box loudspeaker system is a direct-radiator system using an enclosure which has two apertures. One aperture accommodates a driver. The other, called a vent or port, allows air to move in and out of the enclosure in response to the pressure variations within the enclosure.

The vent may be formed as a simple aperture in the enclosure wall or as a tunnel or duct which extends inward from the aperture. In either case, the behavior of the air in the vent is reactive, i.e., it acts as an inertial mass. At low frequencies, the motion of air in the vent contributes substantially to the total volume velocity crossing the enclosure boundaries and therefore to the system output [12].

The analysis of vented-box systems in this paper is essentially an extension of Thiele's approach [10]; it follows the organization of [12] which is in fact a generalized description of Thiele's methods. The principal extensions to Thiele's work include treatment of efficiency–response relationships and large-signal behavior, evaluation of diaphragm–vent interaction, assessment of the magnitude and effects of normal enclosure losses, and calculation of alignment data for systems having such losses. The treatment of enclosure losses is different from that of Nomura [11] because the absorption losses considered by Nomura are found to contribute only a portion of the losses present in practical enclosures.

Some of the analytical results presented in this paper are either obtained or illustrated with the help of an analog circuit simulator similar to that used by Locanthi [2]. Such a simulator is an invaluable aid in the analysis and design of loudspeaker systems because it provides rapid assessment of both time-domain and frequencydomain performance. It is particularly useful in investigating the effects of losses, component tolerances, system misalignment, etc., on response, diaphragm excursion, and voice-coil impedance. It provides results in a fraction of the time that would be required using normal computational methods.

The analytical relationships developed in this paper show that the important performance characteristics of vented-box systems are directly related to a number of basic and easily measured system parameters. Both the assessment and the specification of performance at low frequencies for such systems are therefore relatively simple tasks.

In Parts I and II it is shown that these analytical relationships impose definite quantitative limitations on both small-signal and large-signal performance of vented-box systems and indicate the extent to which the important performance characteristics may be traded off against one another.

In Part III these relationships lead to a method of synthesis (system design) which is free of trial-and-error procedures. This method starts with the desired performance characteristics, checks these for realizability, and results in complete specification of the required system components.

The appendices of the paper are included in Part IV.

2. BASIC ANALYSIS

The impedance-type acoustical analogous circuit of a vented-box loudspeaker system is presented in Fig. 1. This circuit is derived from the generalized circuit of [12, Fig. 2] by short-circuiting the port compliance element. In Fig. 1, the symbols are defined as follows:

- e_g Open-circuit output voltage of source or amplifier
- B Magnetic flux density in driver air gap
- l Length of voice-coil conductor in magnetic field of air gap
- S_D Effective projected surface area of driver diaphragm
- R_g Output resistance of source or amplifier
- R_E Dc resistance of driver voice coil
- C_{AS} Acoustic compliance of driver suspension
- M_{AS} Acoustic mass of driver diaphragm assembly including voice coil and air load
- R_{AS} Acoustic resistance of driver suspension losses
- C_{AB} Acoustic compliance of air in enclosure
- R_{AB} Acoustic resistance of enclosure losses caused by internal energy absorption
- R_{AL} Acoustic resistance of enclosure losses caused by leakage
- M_{AP} Acoustic mass of port or vent including air load
- R_{AP} Acoustic resistance of port or vent losses
- U_D Volume velocity of driver diaphragm
- U_P Volume velocity of port or vent
- U_L Volume velocity of enclosure leakage
- U_B Volume velocity entering enclosure
- U_0 Total volume velocity leaving enclosure boundaries.

This circuit may be simplified to that of Fig. 2 by combining the series resistances in the driver branch to form a single acoustic resistance R_{AT}, where

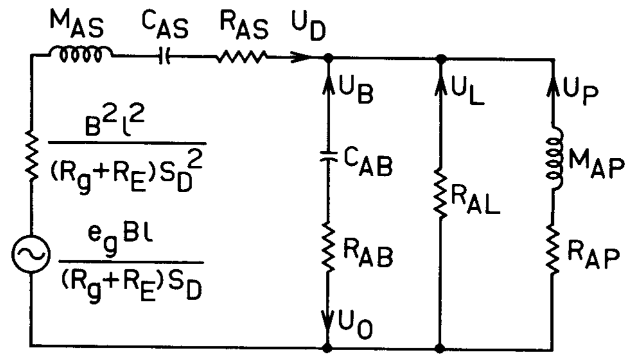

Fig. 1. Acoustical analogous circuit of vented-box loudspeaker system.

$$R_{AT} = R_{AS} + \frac{B^2l^2}{(R_g + R_E) S_D^2} \qquad (1)$$

and by defining

$$p_g = \frac{e_g Bl}{(R_g + R_E) S_D} \qquad (2)$$

as the value of the Thevenin acoustic pressure generator at the left of the circuit. Finally, R_{AB} and R_{AP} are neglected because, as described in the next section, their effects can normally be accounted for by a suitable adjustment to the value of R_{AL}.

By comparison, the circuit used by Novak [7] and Thiele [10] is obtained from that of Fig. 2 by removing the resistance R_{AL}.

The electrical equivalent circuit of the vented-box system is formed by taking the dual of Fig. 1 and converting all impedance elements to their electrical equivalents by the relationship

$$Z_E = B^2l^2/(Z_A S_D^2) \qquad (3)$$

where Z_A is the impedance of an element in the impedance-type acoustical analogous circuit and Z_E is the impedance of the corresponding element in the electrical equivalent circuit. A simplified electrical equivalent circuit corresponding to Fig. 2 is shown in Fig. 3. In this circuit,

- C_{MES} Corresponds to driver mass M_{AS}
- L_{CES} Corresponds to driver suspension compliance C_{AS}
- R_{ES} Corresponds to driver suspension resistance R_{AS}
- L_{CEB} Corresponds to enclosure compliance C_{AB}
- R_{EL} Corresponds to enclosure leakage resistance R_{AL}
- C_{MEP} Corresponds to vent mass M_{AP}.

The circuits presented above are valid only for frequencies within the piston range of the system driver; the element values are assumed to be independent of frequency within this range.

As discussed in [12], the effects of the voice-coil inductance and the resistance of the radiation load are neglected. The effect of external acoustic interaction between driver diaphragm and vent [2], [6] has also been neglected. The reasons for this are given later in the paper.

The analysis of the system and the interpretation of its describing functions are simplified by defining a num-

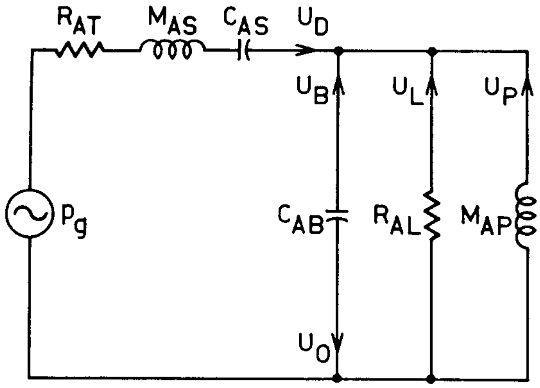

Fig. 2. Simplified acoustical analogous circuit of vented-box loudspeaker system.

ber of component and system parameters. For the enclosure, these are

$$T_B^2 = 1/\omega_B^2 = C_{AB}M_{AP} = C_{MEP}L_{CEB} \tag{4}$$

$$Q_L = \omega_B C_{AB} R_{AL} = 1/(\omega_B C_{MEP} R_{EL}). \tag{5}$$

From Figs. 2 and 3 it can be seen that $\omega_B = 2\pi f_B$ is the resonance frequency of the enclosure–vent circuit, and that Q_L represents the Q of this resonant circuit at ω_B resulting from the leakage losses.

Similarly, the system driver is described by the driver parameters introduced in [12]. These are

$$T_S^2 = 1/\omega_S^2 = C_{AS}M_{AS} = C_{MES}L_{CES} \tag{6}$$

$$Q_{MS} = \omega_S C_{MES} R_{ES} = 1/(\omega_S C_{AS} R_{AS}) \tag{7}$$

$$Q_{ES} = \omega_S C_{MES} R_E = \omega_S R_E M_{AS} S_D^2/(B^2 l^2) \tag{8}$$

$$V_{AS} = \rho_0 c^2 C_{AS}. \tag{9}$$

In Eq. (9) ρ_0 is the density of air (1.18 kg/m^3) and c is the velocity of sound in air (345 m/s). In this paper it is assumed that the values of the first three parameters apply to the driver when the diaphragm air-load mass is that for the driver mounted in the system enclosure [3, pp. 216-217].

The interaction of the source, driver, and enclosure give rise to further system parameters. These are the system compliance ratio α, given by

$$\alpha = C_{AS}/C_{AB} = L_{CES}/L_{CEB} \tag{10}$$

the system tuning ratio h, given by

$$h = f_B/f_S = \omega_B/\omega_S = T_S/T_B \tag{11}$$

and the total Q of the driver connected to the source Q_T, given by

$$Q_T = 1/(\omega_S C_{AS} R_{AT}). \tag{12}$$

Following the method of [12], analysis of the circuits of Figs. 2 and 3 and substitution of the parameters defined above yields the system response function

$$G(s) = \frac{s^4 T_B^2 T_S^2}{s^4 T_B^2 T_S^2 + s^3(T_B^2 T_S/Q_T + T_B T_S^2/Q_L) + s^2[(\alpha+1)T_B^2 + T_B T_S/Q_L Q_T + T_S^2] + s(T_B/Q_L + T_S/Q_T) + 1} \tag{13}$$

where $s = \sigma + j\omega$ is the complex frequency variable, the diaphragm displacement function

$$X(s) = \frac{s^2 T_B^2 + s T_B/Q_L + 1}{D(s)} \tag{14}$$

where $D(s)$ is the denominator of Eq. (13), the displacement constant

$$k_x = 1 \tag{15}$$

and the voice-coil impedance function

$$Z_{VC}(s) = R_E + R_{ES}\frac{s(T_S/Q_{MS})(s^2 T_B^2 + s T_B/Q_L + 1)}{D'(s)} \tag{16}$$

where $D'(s)$ is the denominator of Eq. (13) but with Q_T wherever it appears replaced by Q_{MS}.

3. ENCLOSURE LOSSES

In any vented-box loudspeaker system, three kinds of enclosure losses are present: absorption losses, leakage losses, and vent losses. These losses correpond to the resistances R_{AB}, R_{AL}, and R_{AP} in Fig. 1. The magnitude of each of these losses may be established by defining a value of Q for the enclosure-vent resonant circuit at f_B, considering each loss one at a time. Thus for the leakage losses,

$$Q_L = \omega_B C_{AB} R_{AL} \tag{5}$$

for the absorption losses,

$$Q_A = 1/(\omega_B C_{AB} R_{AB}) \tag{17}$$

and for the vent losses

$$Q_P = 1/(\omega_B C_{AB} R_{AP}). \tag{18}$$

The total Q of the enclosure–vent circuit at f_B is then defined as Q_B, where

$$1/Q_B = 1/Q_L + 1/Q_A + 1/Q_P. \tag{19}$$

It is this Q_B that is measured in a practical system using the method of Thiele described in [10, sec. 14] and in Section 7 (Part II) of this paper.

This paper deals only with systems in which enclosure losses are kept to a practical minimum. Systems making use of deliberately enlarged enclosure losses (e.g., large leaks, resistively damped vents, heavily damped or filled enclosures) will be treated in a later paper.

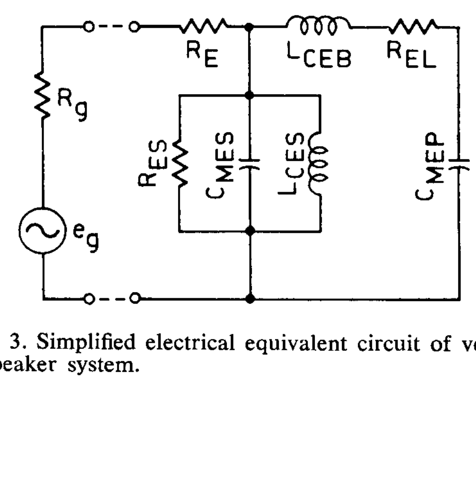

Fig. 3. Simplified electrical equivalent circuit of vented-box loudspeaker system.

Assessment of the contribution of enclosure losses to system performance requires meaningful answers to two questions. First, what is the effect of each kind of loss on system performance? Second, what are the typical magnitudes of the three kinds of losses in practical enclosures?

The answer to the first question has been obtained by constructing the circuit analog of a vented-box system and observing the change in response as a "lossless" enclosure is provided successively with individual leakage, absorption, and vent losses corresponding to a given value of Q. The results for the fourth-order Butterworth (B4) alignment given by Thiele in [10, Table I] are shown in Fig. 4 for Q values of 5. As indicated by Thiele [10, eq. (90)], the maximum response loss occurs at f_B and to a very close approximation depends only on Q_B and not on the actual nature of the loss or losses present. Above f_B absorption losses have the greatest effect and vent losses the least effect on response, while below f_B the relative effects are reversed. The effect of leakage losses is intermediate both above and below f_B. The relative effects are the same for other alignments given in [10], except that, as stated by Thiele, the response loss for a given value of Q_B is greater for alignments having a lower compliance ratio and smaller for alignments having a higher compliance ratio.

The second question has troubled a great many authors because measured losses tend to be higher than the values predicted from theory. Both Beranek [3, p. 257] and Thiele [10, footnote to sec. 14] suspected that absorption losses were to blame for their low measured values of Q_B, and Nomura's paper [11] is based on the assumption that these losses are dominant. Van Leeuwen found that neither lining nor bracing of the enclosure affected his loss measurements [4] and concluded that absorption losses were not significant. He suspected that his extra losses arose in the vent and could be explained only by assuming an increased value for the coefficient of viscosity of air—about 30 times larger than the normally accepted value.

It is possible to determine the magnitude of each kind of loss in practical systems by an extension of Thiele's measurement method as described in Appendix 3. From measurements of this type on a number of commercial and experimental systems, the following was found.

1) Losses in unobstructed vents are usually about the same as or a little greater than the values calculated from viscous theory [10, eq. (7)]. Typical values of Q_P for unobstructed vents are in the range of 50–100. If the vent is obstructed by grill cloth or lining materials, the value of Q_P can fall considerably, but with reasonable care in design need not fall below 20.

2) Absorption losses in unlined enclosures are quite small, giving Q_A values of 100 or more. Typical lining materials placed on the enclosures walls where air particle velocity is low do not extract very much energy [13, p. 383] but can reduce Q_A to a range of 30–80. Very thick linings or damping partitions reduce Q_A even further.

3) Leakage losses are usually the most significant, giving Q_L values of between 5 and 20.

The last result is surprising, because the enclosures tested were well built and appeared to be quite leak-free. In fact, some of the more serious leaks were traced to the drivers. These leaks were caused by imperfect gasket seals and/or by leakage of air through a porous dust cap and past the voice coil. However, the few systems having drivers with solid dust caps and perfect gaskets still had dominant measured leakage losses.

Confidence in the measurement method, based on its ability to detect with reasonable accuracy the deliberate introduction of small additional enclosure losses, leads to the conclusion that the measured leakage in apparently leak-free systems is not an error of measurement but an indication that the actual losses in the system enclosure are not constant with frequency as assumed in the method of measurement (Appendix 3).

The analog circuit simulator has proved to be an invaluable aid in reaching and supporting this conclusion and also in establishing the practical meaning and usefulness of the total-loss measurement. First, it has shown that vent losses which increase with frequency and absorption losses which decrease with frequency do indeed appear in the measurement results as apparent leakage. Second, it has shown that where such frequency-varying losses are present, the system response is predicted with extremely high accuracy from the measured values of Q_A, Q_L, and Q_P as defined.

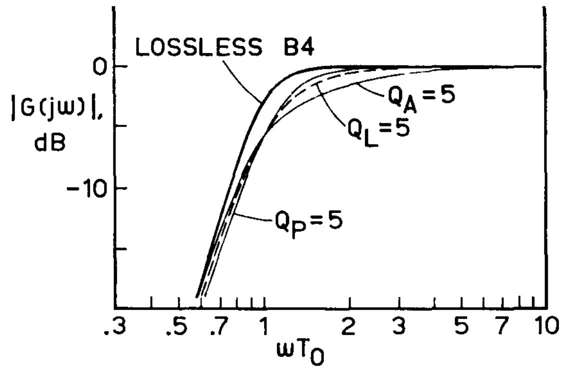

Fig. 4. Effects of enclosure-circuit losses on response of a lossless B4-aligned vented-box loudspeaker system (from simulator).

Finally, and not surprisingly in view of Fig. 4, it has shown that approximately equal values of Q_A and Q_P in the range of values normally measured in practical enclosures have a combined effect on system response which is effectively indistinguishable from the same total value of Q_L.

The above findings lead to the conclusion that even where *actual* leakage is not dominant, the enclosure losses present in a normal vented-box system may be adequately approximated, for purposes of evaluation or design, by a single frequency-invariant leakage resistance. The value of this equivalent leakage resistance is such that the corresponding value of Q_L is equal to the total Q_B that would be measured in the real system by Thiele's method. This approximation is reflected in Figs. 2 and 3 and in the system describing functions Eqs. (13), (14), and (16).

4. RESPONSE

Response Function

The response function of the vented-box system is given by Eq. (13). This is a fourth-order (24-dB per

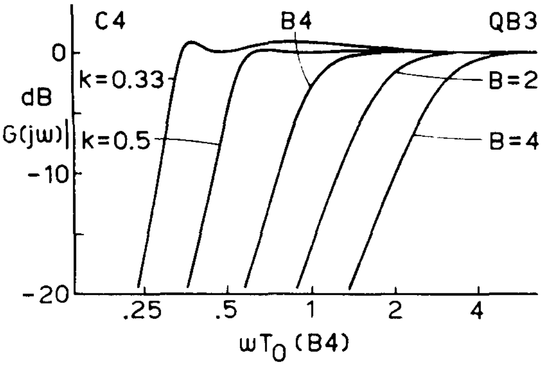

Fig. 5. Normalized response curves for B4 and selected C4 and QB3 alignments of vented-box loudspeaker system.

octave cutoff) high-pass filter function which may be expressed in the general form

$$G(s) = \frac{s^4T_0{}^4}{s^4T_0{}^4 + a_1s^3T_0{}^3 + a_2s^2T_0{}^2 + a_3sT_0 + 1} \tag{20}$$

where T_0 is the nominal filter time constant and a_1, a_2, a_3 are coefficients which determine the behavior of the filter response.[1]

The behavior of Eq. (13) may be assessed by studying Eq. (20) and then using the relationships which make the corresponding terms of the two expressions identical. Using Eq. (11), these are

$$T_0 = (T_BT_S)^{1/2} = T_S/h^{1/2} \tag{21}$$

$$a_1 = \frac{Q_L + hQ_T}{h^{1/2}Q_LQ_T} \tag{22}$$

$$a_2 = \frac{h + (\alpha + 1 + h^2)Q_LQ_T}{hQ_LQ_T} \tag{23}$$

$$a_3 = \frac{hQ_L + Q_T}{h^{1/2}Q_LQ_T}. \tag{24}$$

Frequency Response

Alignment

The frequency response $|G(j\omega)|$ of Eq. (20) is examined in Appendix 1. Coefficient data are given for a variety of useful response characteristics which may be used to align the vented-box system.

Three very useful types of alignments are given by Thiele in [10]. These are the fourth-order Butterworth maximally flat alignment (B4), the fourth-order Chebyshev equal-ripple alignment (C4), and the alignment which Thiele has dubbed "quasi-third-order Butterworth" (QB3). Alternative alignments include the degenerated Chebyshev responses of Nomura [11] and the sub-Chebyshev responses of Thiele [14], although the latter provide less effective use of enclosure volume in relation to the efficiency and low-frequency cutoff obtained, i.e., a lower value of the efficiency constant described in Section 5.

[1] This normalization of the filter function follows the example of Thiele [10]. The relationships between this form of normalization and others, e.g., that used by Weinberg [18], including relative pole locations are given by Benson in [32, pp. 422-438 and Appendix 7].

Both the C4 and QB3 alignments provide a wide range of realizable response characteristics with gradually changing properties. Also, both as a limiting case coincide with the unique B4 alignment, so a completely continuous span of alignments is mathematically possible. A few of these alignments are illustrated in Fig. 5. The frequency scale of Fig. 5 is normalized to the nominal time constant of the B4 alignment; the other curves are plotted to the same scale but displaced horizontally for clarity. In this paper, the C4 alignments are specified by the value of k used by Thiele and defined in Appendix 1. The QB3 alignments are specified by the value of B defined in Appendix 1.

Inspection of Eqs. (21–24) reveals that the four mathematical variables needed to specify a given alignment, T_0, a_1, a_2, and a_3, are related to five independent system variables (or parameters), T_S, h, α, Q_L, and Q_T. This means that specification of a particular alignment does not correspond to a unique set of system parameters but may be obtained in a variety of ways. For any given alignment, one parameter may be assigned arbitrarily (within limits of realizability) and the rest may then be calculated.

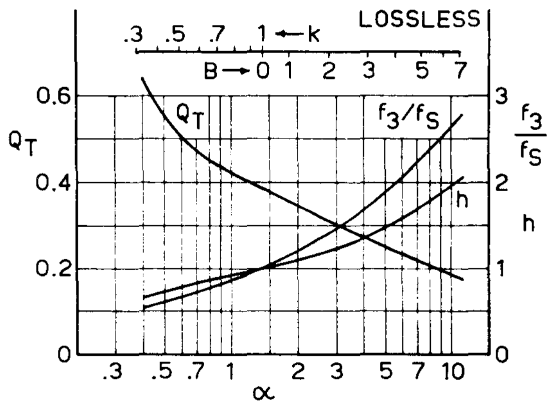

Fig. 6. Alignment chart for lossless vented-box systems.

A basic understanding of the behavior of the vented-box system is quickly obtained if the enclosure losses are ignored, i.e., Q_L is taken to be infinite. In this case, Eqs. (22–24) are simplified and all alignments become unique in terms of the system parameters. This is the process followed by Thiele in [10].

Fig. 6 is an alignment chart for systems with lossless enclosures based on the C4, B4, and QB3 alignments. The compliance ratio α is chosen as the primary independent variable and plotted as the abscissa of the figure. The corresponding values of k and B which specify the C4 and QB3 alignments are also given on the figure. Because each alignment is unique, every value of α corresponds to a specific alignment and requires specific values of the other system parameters to obtain the correct response. Thus the figure gives the values of Q_T and the tuning ratio $h = f_B/f_S$ required for each value of α, as well as the normalized cutoff frequency f_3/f_S at which the response is 3 dB down from its high-frequency asymptotic value.

Misalignment

The effect of an incorrectly adjusted parameter on the

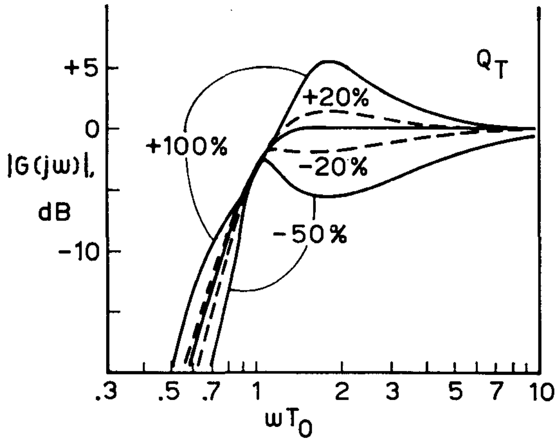

Fig. 7. Variations in frequency response of lossless B4-aligned vented-box system for misalignment of Q_T (from simulator).

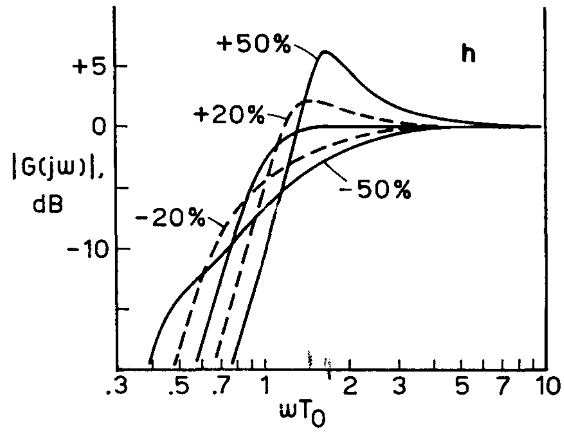

Fig. 8. Variations in frequency response of lossless B4-aligned vented-box system for misalignment of h (from simulator).

frequency response of a vented-box system is easily observed using the analog circuit simulator. Fig. 7 shows the variation produced in the response of a lossless system aligned for a B4 response by changes in the value of Q_T of $\pm 20\%$, -50%, and $+100\%$. This agrees exactly with [10, eqs. (42) and (43)] which indicate that the response at the frequencies f_L and f_H of the voice-coil impedance peaks is directly proportional to Q_T, while the response at f_B is independent of Q_T. Fig. 8 shows the variations produced in the same alignment by mistuning (changing the value of h) of $\pm 20\%$ and $\pm 50\%$.

Similar effects occur with other alignments. It is not difficult to see why the vented enclosure is sometimes scorned as a "boom box" when it is realized that the values of Q_T required are much lower than the majority of woofers provide [15, Table 13] and that a historical emphasis on unity tuning ratio regardless of compliance ratio often results in erroneously high tuning.

Alignment with Enclosure Losses

Using the approximation arrived at in Section 3, the parameter relationships required to provide a specified response in the presence of enclosure losses may be calculated as described in Appendix 1. Compared to lossless alignments, a particular response characteristic generally requires a larger value of Q_T and a smaller value of α.

Alignment charts for the C4, B4, and QB3 responses are presented in Figs. 9–13 for systems having enclosure losses corresponding to a Q_L of 20, 10, 7, 5, and 3, respectively. These values are representative of real enclosures, for which the most commonly measured values of Q_B are in the range of 5–10.

Transient Response

Keibs [8], [16] offered alignment solutions for what he considered to be the optimum transient response of a fourth-order filter. The same alignment parameters were later advocated by Novak [17]. The step responses of various fourth-order high-pass filter alignments are illustrated in Fig. 14. The alignments range from Chebyshev to sub-Chebyshev types and include the alignment recommended by Keibs.

The transient response of any minimum-phase network is of course directly related to the frequency response. For the vented-box system, the alignments which have more gradual rolloff also have less violent transient ringing. If transient response is considered important, then it would appear that the QB3 alignments are to be preferred over the B4 and C4 alignments. The SC4 alignments (Appendix 1) provide a further improvement in

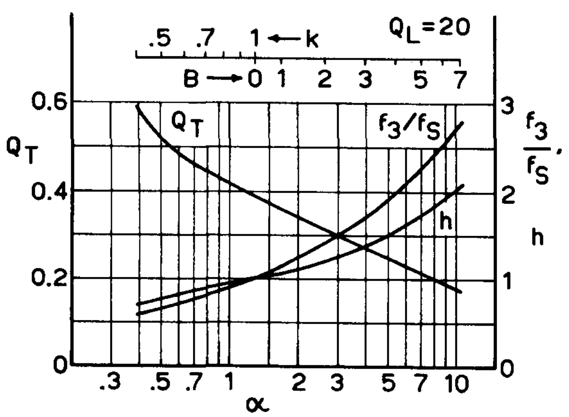

Fig. 9. Alignment chart for vented-box systems with $Q_B = Q_L = 20$.

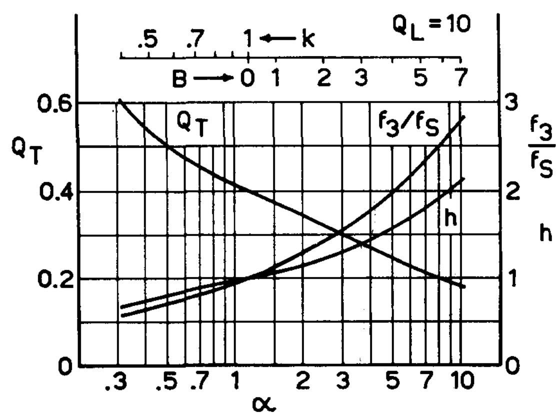

Fig. 10. Alignment chart for vented-box systems with $Q_B = Q_L = 10$.

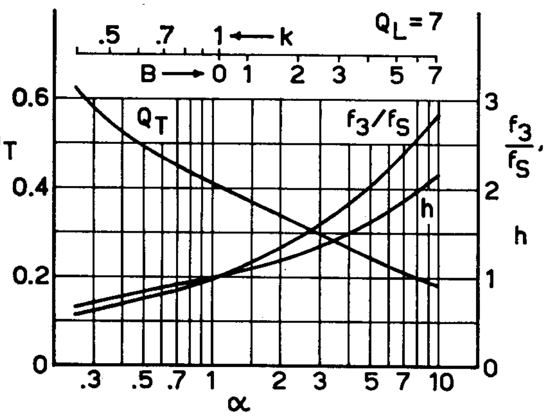

Fig. 11. Alignment chart for vented-box systems with $Q_B = Q_L = 7$.

transient response but have a less attractive frequency response.

Phase and Delay Response

Weinberg [18] shows how the conditions of maximal flatness or equal-ripple behavior may be imposed on any property of a response function, including phase response and group delay. The condition of maximally flat passband group delay is provided by the Bessel filter. The polynomial coefficients of the fourth-order Bessel filter are calculated in Appendix 1 from the pole locations given in [19].

General Response Realization

Any physically realizable minimum-phase fourth-order response characteristic which can be described in terms of the coefficients of Eq. (20) can be realized in a vented-box loudspeaker system. Using the method of Appendix 1, the coefficients may be processed into system alignment parameters which will produce the specified response.

5. EFFICIENCY

Reference Efficiency

The piston-range reference efficiency of a vented-box loudspeaker system is the reference efficiency of the system driver when the total air-load mass seen by the driver diaphragm is the same as that imposed by

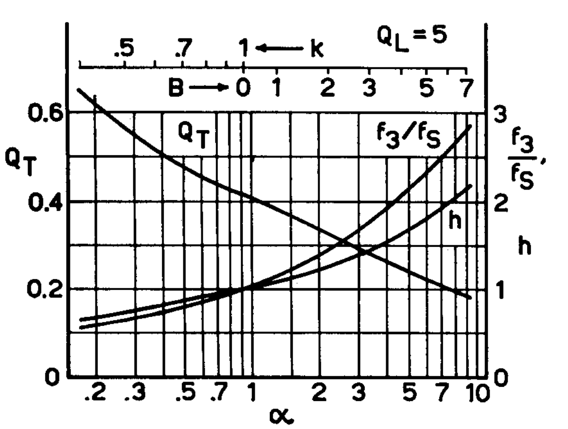

Fig. 12. Alignment chart for vented-box systems with $Q_B = Q_L = 5$.

the enclosure. Thus if the driver parameters are measured under or adjusted to correspond to this condition, the system reference efficiency η_0 is [12, eq. (32)]

$$\eta_0 = \frac{4\pi^2}{c^3} \cdot \frac{f_S{}^3 V_{AS}}{Q_{ES}}. \tag{25}$$

For SI units, the value of $4\pi^2/c^3$ is 9.64×10^{-7}.

Efficiency Factors

Eq. (25) may be written

$$\eta_0 = k_\eta f_3{}^3 V_B \tag{26}$$

where f_3 is the cutoff (half-power or -3 dB) frequency of the system, V_B is the net internal volume of the system enclosure, and $k\eta$ is an efficiency constant given by

$$k_\eta = \frac{4\pi^2}{c^3} \cdot \frac{V_{AS}}{V_B} \cdot \frac{f_S{}^3}{f_3{}^3} \cdot \frac{1}{Q_{ES}}. \tag{27}$$

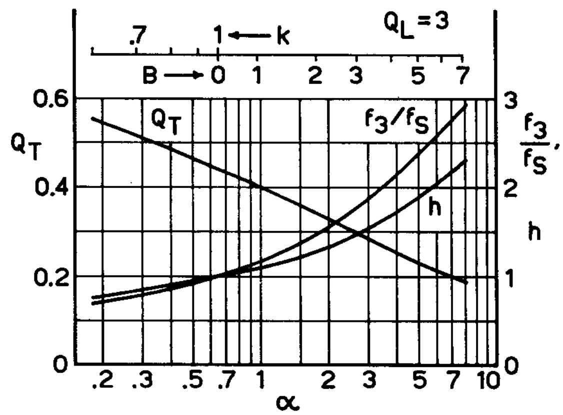

Fig. 13. Alignment chart for vented-box systems with $Q_B = Q_L = 3$.

The efficiency constant k_η may be separated into two factors, $k_{\eta(Q)}$ related to driver losses and $k_{\eta(G)}$ related to the response characteristic and enclosure losses. Thus,

$$k_\eta = k_{\eta(Q)} k_{\eta(G)} \tag{28}$$

where

$$k_{\eta(Q)} = Q_T/Q_{ES} \tag{29}$$

$$k_{\eta(G)} = \frac{4\pi^2}{c^3} \cdot \frac{V_{AS}}{V_B} \cdot \frac{f_S{}^3}{f_3{}^3} \cdot \frac{1}{Q_T}. \tag{30}$$

Driver Loss Factor

The value of Q_T for systems used with modern high-damping-factor amplifiers ($R_g = 0$) is equal to Q_{TS}, where [12, eq. (47)]

$$Q_{TS} = \frac{Q_{ES} Q_{MS}}{Q_{ES} + Q_{MS}}. \tag{31}$$

Eq. (29) then reduces to

$$k_{\eta(Q)} = Q_{TS}/Q_{ES} = 1 - Q_{TS}/Q_{MS}. \tag{32}$$

This expression has a maximum value of unity which is approached only when mechanical driver losses are negligible (Q_{MS} infinite) and all required damping is

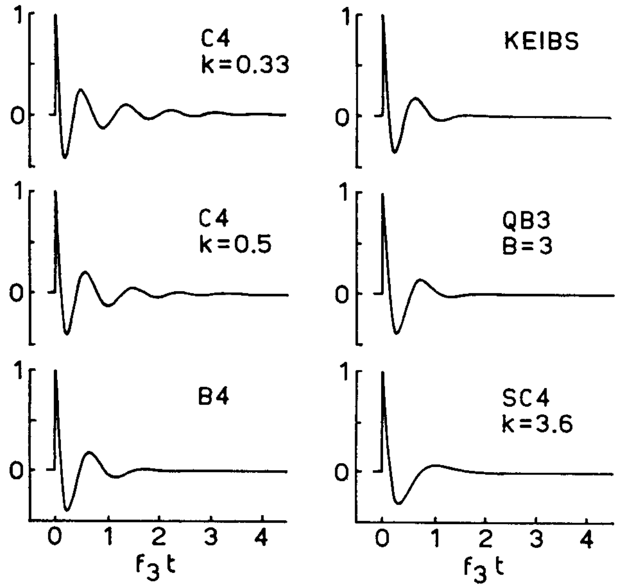

Fig. 14. Normalized step response of vented-box loudspeaker system (from simulator).

provided by electromagnetic coupling ($Q_{ES} = Q_{TS}$).

The value of $k_{\eta(Q)}$ for typical vented-box system drivers is in the range of 0.8–0.95.

System Response Factor

Normally, vented enclosures contain only a small amount of damping material used as a lining. Under these conditions [3, p. 129],

$$C_{AB} = V_B/\rho_0 c^2 \qquad (33)$$

and, using Eqs. (9) and (10), Eq. (30) can be written in terms of the system parameters as

$$k_{\eta(G)} = \frac{4\pi^2}{c^3} \cdot \frac{\alpha}{Q_T (f_3/f_S)^3}. \qquad (34)$$

The relationships between α, Q_T, and f_3/f_S for the C4–B4–QB3 alignments have already been calculated and plotted in Figs. 6 and 9–13. Thus the value of $k_{\eta(Q)}$ for any of these alignments can also be calculated. Fig. 15 is a plot of the value of $k_{\eta(G)}$ as a function of α for several values of Q_L. For reference, the location

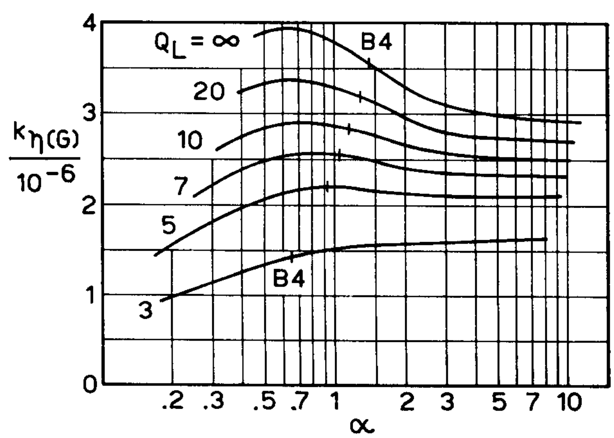

Fig. 15. Response factor $k_{\eta(G)}$ of efficiency constant for vented-box loudspeaker system as a function of α (system compliance ratio) for several values of enclosure Q.

of the B4 alignment is indicated on each curve by a short vertical bar.

It is clear that enclosure losses significantly reduce the value of $k_{\eta(G)}$ for a correctly aligned system. The maximum possible value of $k_{\eta(G)}$ is 3.9×10^{-6} and occurs when the enclosure losses are negligible and the system compliance ratio is adjusted to about 0.6. This is a $k = 0.5$ C4 alignment which has a ripple of about 0.2 dB.

Maximum Reference Efficiency, Cutoff Frequency, and Enclosure Volume

Taking the maximum theoretical values of $k_{\eta(Q)}$ and $k_{\eta(G)}$, the maximum reference efficiency $\eta_{0(\max)}$ that could be obtained from a lossless vented-box system for specified values of f_3 and V_B is, from Eqs. (26) and (28),

$$\eta_{0(\max)} = 3.9 \times 10^{-6} f_3^3 V_B \qquad (35)$$

with f_3 in Hz and V_B in m^3. This relationship is illustrated in Fig. 16, with V_B (given here in cubic decimeters: 1 dm^3 = 1 liter = 10^{-3} m^3) plotted against f_3 for various values of $\eta_{0(\max)}$ expressed in percent.

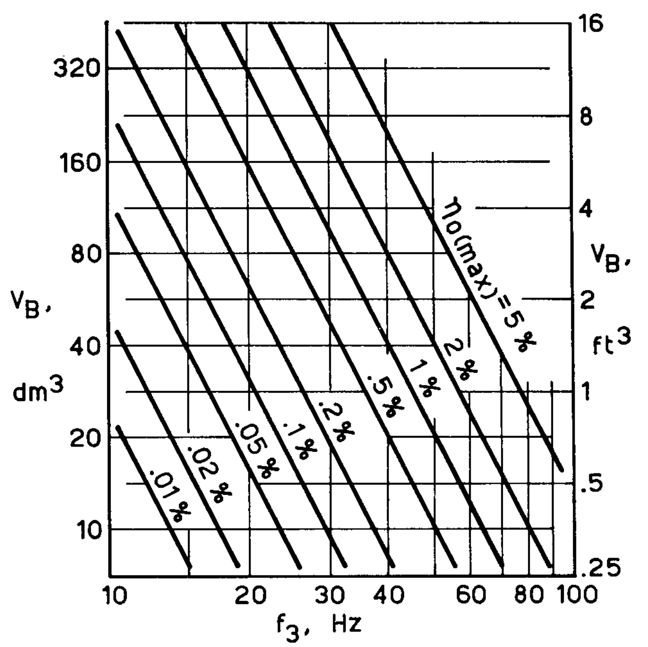

Fig. 16. Relationship between cutoff frequency, enclosure volume, and maximum reference efficiency for vented-box loudspeaker system.

Fig. 16 represents the physical efficiency–cutoff frequency–volume limitation of vented-box system design. A practical system having given values of f_3 and V_B must always have an actual reference efficiency lower than the corresponding value of $\eta_{0(\max)}$ given by Fig. 16. Similarly, a system of specified efficiency and volume must have a cutoff frequency higher than that indicated by Fig. 16, and so on.

Actual vented-box systems have an efficiency lower than the maximum given by Eq. (35) because of driver mechanical losses, enclosure losses, and the use of alignments other than that which gives maximum efficiency for a given value of Q_L. Typical practical efficiencies are 40–50% (2–3 dB) lower than the theoretical maximum given by Eq. (35) or Fig. 16. For most systems, the driver parameters can be measured and the reference efficiency calculated directly from Eq. (25).

The physical limitation imposed by Eq. (35) or Fig. 16 may be overcome in a sense by the use of amplifier assistance, i.e., networks which raise the gain of the amplifier in the cutoff region of the system [10], [20]. While the overall response of the complete system is thus extended, there is no change in the driver-enclosure efficiency in the cutoff region. The amplifier must deliver more power, and the driver must dissipate this power.

REFERENCES—PART I

[1] A. L. Thuras, "Sound Translating Device," U.S. Patent No. 1,869,178, application Aug. 15, 1930, patented July 26, 1932.

[2] B. N. Locanthi, "Application of Electric Circuit Analogies to Loudspeaker Design Problems," *IRE Trans. Audio,* vol. PGA-6, p. 15 (Mar. 1952); republished in *J. Audio Eng. Soc.,* vol. 19, p. 778 (Oct. 1971).

[3] L. L. Beranek, *Acoustics* (McGraw-Hill, New York, 1954).

[4] F. J. van Leeuwen, "De Basreflexstraler in de Akoestiek," *Tijdschrift Nederlands Radiogenootschap,* vol. 21, p. 195 (Sept. 1956).

[5] E. de Boer, "Acoustic Interaction in Vented Loudspeaker Enclosures," *J. Acoust. Soc. Amer.* (Letter) vol. 31, p. 246 (Feb. 1959).

[6] R. H. Lyon, "On the Low-Frequency Radiation Load of a Bass-Reflex Speaker," *J. Acoust. Soc. Amer.* (Letter), vol. 29, p. 654 (May 1957).

[7] J. F. Novak, "Performance of Enclosures for Low-Resonance High-Compliance Loudspeakers," *IRE Trans. Audio,* vol. AU-7, p. 5 (Jan./Feb. 1959); also *J. Audio Eng. Soc.,* vol. 7, p. 29 (Jan. 1959).

[8] L. Keibs, "The Physical Conditions for Optimum Bass Reflex Cabinets," *J. Audio Eng. Soc.,* vol. 8, p. 258 (Oct. 1960).

[9] E. de Boer, "Synthesis of Bass-Reflex Loudspeaker Enclosures," *Acustica,* vol. 11, p. 1 (1961).

[10] A. N. Thiele, "Loudspeakers in Vented Boxes," *Proc. IREE (Australia),* vol. 22, p. 487 (Aug. 1961); republished in *J. Audio Eng. Soc.,* vol. 19, p. 382 (May 1971) and p. 471 (June 1971).

[11] Y. Nomura, "An Analysis of Design Conditions of a Bass-Reflex Loudspeaker Enclosure for Flat Response," *Electron. Commun. Japan,* vol. 52-A, no. 10, p. 1 (1969).

[12] R. H. Small, "Direct-Radiator Loudspeaker System Analysis," *IEEE Trans. Audio Electroacoust.,* vol. AU-19, p. 269 (Dec. 1971); republished in *J. Audio Eng. Soc.,* vol. 20, p. 383 (June 1972).

[13] D. E. L. Shorter, "Loudspeaker Cabinet Design," *Wireless World,* vol. 56, p. 382 (Nov. 1950), and p. 436 (Dec. 1950).

[14] A. N. Thiele, "Filters with Variable Cut-off Frequencies," *Proc. IREE (Australia),* vol. 26, p. 284 (Sept. 1965).

[15] J. R. Ashley and M. D. Swan, "Improved Measurement of Loudspeaker Driver Parameters," presented at the 40th Convention of the Audio Engineering Society, Los Angeles (Apr. 1971), Preprint 803.

[16] B. C. Reith, "Bass-Reflex Enclosures," *Wireless World,* (Letter), vol. 73, p. 38 (Jan. 1967).

[17] J. F. Novak, "Designing a Ducted-Port Bass-Reflex Enclosure," *Electron. World,* vol. 75, p. 25 (Jan. 1966).

[18] L. Weinberg, *Network Analysis and Synthesis* (McGraw-Hill, New York, 1962), ch. 11.

[19] R. M. Golden and J. F. Kaiser, "Root and Delay Parameters for Normalized Bessel and Butterworth Low-Pass Transfer Functions," *IEEE Trans. Audio Electroacoust.,* vol. AU-19, p. 64 (Mar. 1971).

[20] A. N. Thiele, "Equalisers for Loudspeakers," presented at the 12th National Convention of the IREE (Australia), (May 1969).

[32] J. E. Benson, "Theory and Design of Loudspeaker Enclosures, Part 3—Introduction to Synthesis of Vented Systems," *A.W.A. Tech. Rev.,* vol. 14, p. 369 (Nov. 1972).

Editor's Note: Dr. Small's biography appeared in the December issue.

Vented-Box Loudspeaker Systems Part II: Large-Signal Analysis

RICHARD H. SMALL

School of Electrical Engineering, The University of Sydney, Sydney, N.S.W. 2006, Australia

The power capacity of a vented-box loudspeaker system is shown to be directly related to the system frequency response and to the volume of air that can be displaced by the system driver. The vent area must be made large enough to prevent noise generation or excessive losses; the required area is shown to be quantitatively related to enclosure tuning and to driver displacement volume. Mutual coupling between driver and vent is found to be of negligible importance in most cases.

The basic performance characteristics of a vented-box system may be determined from knowledge of a number of fundamental system parameters. These parameters can be evaluated from relatively simple measurements. The vented-box system is shown to possess two important performance advantages compared with the closed-box system.

Editor's Note: Part I of Vented-Box Loudspeaker Systems appeared in the June issue.

6. DISPLACEMENT-LIMITED POWER RATINGS

Diaphragm Displacement

The vented-box system displacement function given by Eq. (14) is a low-pass filter function which has a notch at f_B contributed by the numerator and an ultimate cutoff slope of 12 dB per octave at high frequencies. The behavior of this function is examined at the end of Appendix 1.

The normalized diaphragm displacement magnitude $|X(j\omega)|$ is plotted in Fig. 17 for a few common alignments. For convenience, the frequency scale is normalized to f_B. Note that the effect of moving from the C4 alignments toward the QB3 alignments (i.e., increasing a) is to reduce the diaphragm displacement near and above f_B relative to the displacement at zero frequency, and that the principal effect of enclosure losses is to increase the displacement near f_B, i.e., reduce the sharpness of the notch.

Acoustic Power Rating

Assuming linear large-signal diaphragm displacement, the steady-state displacement-limited acoustic power rating P_{AR} of a loudspeaker system, from [12, eq. (42)], is

$$P_{AR} = \frac{4\pi^3 \rho_0}{c} \cdot \frac{f_S^4 V_D^2}{k_x^2 |X(j\omega)|_{\max}^2} \tag{36}$$

where $|X(j\omega)|_{\max}$ is the maximum magnitude attained by the displacement function and V_D is the peak displacement volume of the driver diaphragm, given by

$$V_D = S_D x_{\max} \tag{37}$$

x_{max} being the peak linear displacement of the driver diaphragm, usually set by the amount of voice-coil overhang.

For the vented-box system, Eq. (15) gives $k_x = 1$. The displacement-limited acoustic power rating of the vented-box system then becomes

$$P_{AR(VB)} = \frac{4\pi^3\rho_0}{c} \cdot \frac{f_S^4 V_D^2}{|X(j\omega)|_{max}^2}. \tag{38}$$

For SI units, the value of $4\pi^3\rho_0/c$ is 0.424.

Power-Rating Constant

Eq. (38) may be written in the form

$$P_{AR(VB)} = k_P f_3^4 V_D^2 \tag{39}$$

where k_P is a power-rating constant given by

$$k_P = \frac{4\pi^3\rho_0}{c} \cdot \frac{1}{(f_3/f_S)^4 |X(j\omega)|_{max}^2}. \tag{40}$$

The value of f_3/f_S is already established for any alignment in the C4–B4–QB3 range. But from Fig. 17, $|X(j\omega)|$ has *two* maxima. The first occurs outside the system passband; this has a value of unity and is located at zero frequency for the QB3, B4, and moderate C4 alignments but slightly exceeds unity and is located below f_B for the extreme C4 alignments. The second maximum occurs within the system passband, above f_B, and is always smaller than the first.

There are thus two possible values for k_P, one if the system driving signal is allowed to have large-amplitude components at frequencies well below cutoff, and another, which is substantially larger, if the signal is restricted so that all significant spectral components are within the system passband.

Fig. 18 is a plot of the values of k_P for each of the above driving conditions as a function of the alignment parameters k and B for systems with lossless enclosures. The crosses in Fig. 18 indicate the values of k_P for a few selected alignments with $Q_L = 5$. The effect of this relatively severe amount of enclosure loss on k_P is negligible for the QB3 alignments but gradually increases as the extreme C4 alignments are approached. For these alignments, k_P is slightly reduced for the passband-drive case but slightly increased for the wideband-drive case.

Program Acoustic Power Rating

In most program applications, a portion of the driving signal spectrum lies below the system passband. The lower value of k_P given by Fig. 18 is then in general conservative, while the higher value is comparatively optimistic. A truly realistic value of k_P for program material can be evaluated only if the actual spectral power distribution of the particular driving signal is known. Thiele for example has obtained comparative power handling data for a number of system alignments (including amplifier-assisted alignments) based on a particular random-noise driving signal [20].

In most cases, provided that the program spectrum is principally within the system passband, a satisfactory program rating is obtained by setting k_P equal to 3.0, regardless of the alignment used. This is indicated by the broken line in Fig. 18. This compromise value for k_P is arrived at by considering, for the entire range of alignments, the passband and wideband values of k_P, the ratio of maximum displacements for passband- and wideband-drive conditions, and the degree to which the driving signal spectrum may extend below system cutoff before the displacement exceeds the passband maximum (see Fig. 17).

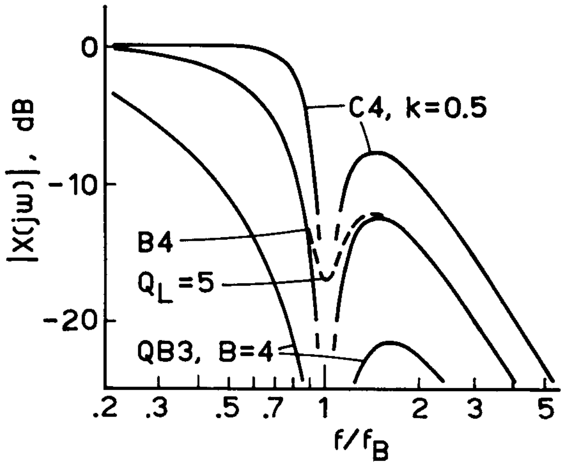

Fig. 17. Normalized diaphragm displacement of vented-box system driver as a function of normalized frequency for several typical alignments (from simulator).

With this value of k_P, Eq. (39) becomes

$$P_{AR(VB)} = 3.0 f_3^4 V_D^2. \tag{41}$$

This relationship is generally applicable to all vented-box alignments for which the system passband includes the major components of the program signal spectrum. Whenever the signal and alignment properties are accurately known, a more exact relationship may be obtained with the help of Fig. 18 or by using Eq. (38) directly.

Power Output, Cutoff Frequency, and Displacement Volume

Eq. (41) is illustrated in Fig. 19. P_{AR} is expressed in both watts (left scale) and equivalent sound pressure

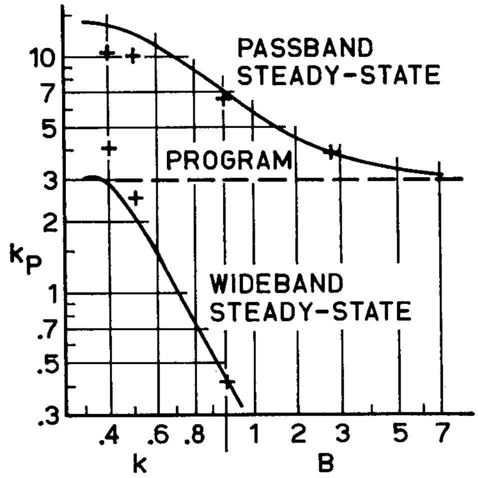

Fig. 18. Power rating constant k_P for vented-box loudspeaker system as a function of response shape. Solid lines are for lossless systems; crosses represent systems with $Q_L = 5$.

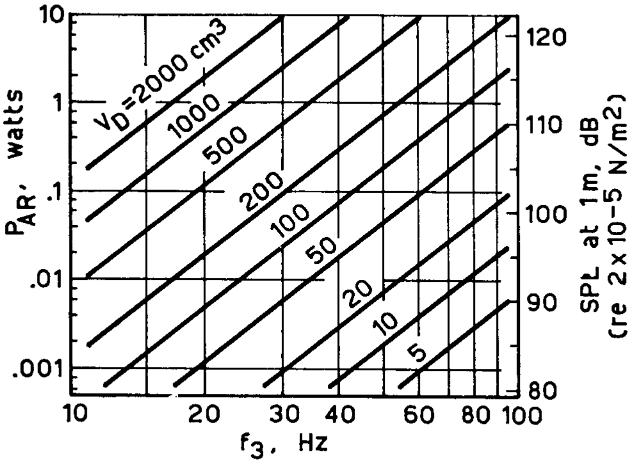

Fig. 19. Relationship between cutoff frequency, driver displacement volume, and rated acoustic power for a vented-box loudspeaker system operated on program material.

level (SPL) at 1 meter [3, p. 14] for 2π-steradian free-field radiation conditions (right scale). This is plotted as a function of f_3 for various values of V_D (note 1 cm^3 = 10^{-6} m^3). The SPL at 1 meter given on the right-hand scale is a rough indication of the SPL produced in the reverberant field of an average listening room for a radiated acoustic power given by the left-hand scale [3, p. 318]. For particular listening environments such as large halls, the reference just cited gives methods for computing the acoustic power required to obtain a specified SPL.

Fig. 19 represents the approximate physical large-signal limitation of vented-box system design. It may be used to determine the maximum performance tradeoffs (P_{AR} versus f_3) for a given voice-coil/suspension design or to find the minimum value of V_D which is required to meet a given specification of f_3 and P_{AR}.

Power ratings calculated from Eq. (41) or Fig. 19 apply only for "typical" program material which does not drive the system hard at frequencies below cutoff. For other circumstances the applicable rating may be higher or lower. Even where the condition of passband drive is met with regard to the intended program material, the vented-box system is clearly vulnerable to extraneous signals such as turntable rumble and subsonic control tones. These normally inaudible signals may produce audible harmonics or cause noticeable modulation distortion [21]. In cases where such signals are particularly troublesome and cannot otherwise be eliminated, the use of a closed-box design or one of the higher order amplifier-assisted vented-box alignments described by Thiele [10], [20] may provide relief.

Electrical Power Rating

The displacement-limited electrical power rating P_{ER} of the vented-box system is obtained by dividing the acoustic power rating Eq. (38) by the system reference efficiency Eq. (25). Thus,

$$P_{ER(VB)} = \frac{P_{AR(VB)}}{\eta_0} = \pi\rho_0 c^2 \frac{f_S Q_{ES}}{V_{AS}} \cdot \frac{V_D^2}{|X(j\omega)|_{\max}^2}. \quad (42)$$

This rating is subject to the same adjustments for program material as used above. Its dependence on the performance factors already discussed is easily observed from the form obtained by dividing Eq. (39) by Eq. (26):

$$P_{ER} = \frac{k_P}{k_\eta} f_3 \frac{V_D^2}{V_B}. \quad (43)$$

In practice, the values of P_{AR} and η_0 are much more important; these would normally be specified or calculated first. P_{ER} is then obtained directly from these numbers as indicated by Eq. (42). P_{ER} describes only the amount of nominal power which may be absorbed from an amplifier if thermal design of the voice-coil permits. It gives no indication of acoustic performance unless reference efficiency is known.

Enclosure and driver losses reduce η_0 without much effect on P_{AR} and thus lead to a higher value of P_{ER}. Driver displacement nonlinearity for large signals also has the effect of reducing efficiency at high levels, i.e., increasing the electrical input required to actually reach the driver displacement limit. In both cases, the extra input power is only dissipated as heat.

7. PARAMETER MEASUREMENT

The direct dependence of system performance characteristics on system parameters provides a simple means of assessing or predicting loudspeaker system performance from a knowledge of these parameters. The important small-signal parameters can be found with satisfactory accuracy from measurement of the voice-coil impedance of the system and its driver.

The voice-coil impedance function of the vented-box system is given by Eq. (16). A plot of the steady-state magnitude $|Z_{VC}(j\omega)|$ of this function against frequency has the shape illustrated in Fig. 20; the measured impedance curve of a practical vented-box system has this same characteristic shape.

The impedance magnitude plot of Fig. 20 has a minimum at a frequency near f_B (labeled f_M) where the impedance magnitude is somewhat greater than R_E. The additional resistance is contributed primarily by enclosure losses and is designated R_{BM} on the plot axis. There are two maxima in the impedance plot, located at frequencies below and above f_M. These are labeled f_L and f_H. At these frequencies, the magnitudes of the impedance maxima depend on both driver losses and enclosure circuit losses and are seldom equal.

Where only normal enclosure losses are present, the basic system parameters and the total enclosures loss Q_B may be found with satisfactory accuracy using the method developed by Thiele in [10]. The indicated value of Q_B may then be used to check the measurement approximations. Thiele's method is based on an initial assumption of negligible enclosure losses and may be summarized as follows. The relationships are derived in Appendix 2.

1) Measure the three frequencies f_L, f_M, and f_H where the impedance magnitude is maximum or minimum. The accurate identification of these frequencies may be aided by measuring the impedance phase; if this passes through zero at the appropriate maximum or minimum, the frequency of zero phase (which may be located with high precision) may be taken as the center of the maximum or minimum. However, if zero phase is not closely coincident with maximum or minimum magnitude, as may occur for moderate to high enclosure losses, the frequency of actual maximum or minimum impedance mag-

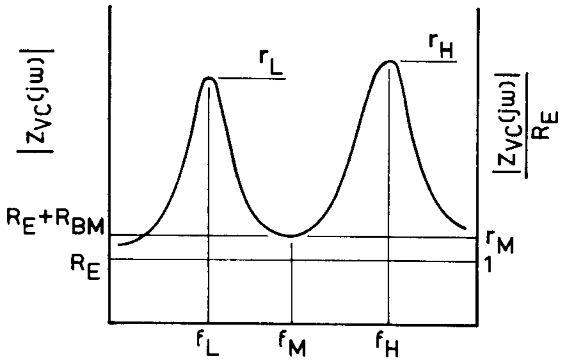

Fig. 20. Voice-coil impedance magnitude of vented-box loudspeaker system as a function of frequency.

nitude must be located as carefully as possible. Experience with many systems and experiments with the analog circuit simulator have shown that where the frequencies of zero phase and maximum or minimum magnitude do not coincide, the latter always provide more accurate values of the system parameters. Bypass any crossover networks for this measurement, and keep the measuring signal small enough so that both voltage and current signals are undistorted sinusoids. For the following calculations, assume that $f_B = f_M$.[2]

2) Calculate f_{SB}, the resonance frequency of the driver for the air-load mass presented by the enclosure, from the relationship

$$f_{SB} = \frac{f_L f_H}{f_B}. \tag{44}$$

3) Calculate the compliance ratio α from the relationship

$$\alpha = \frac{(f_H + f_B)(f_H - f_B)(f_B + f_L)(f_B - f_L)}{f_H^2 f_L^2}. \tag{45}$$

If the enclosure contains little or no lining material, the driver compliance equivalent volume V_{AS} may be calculated in terms of the enclosure net volume V_B. The relationship is, from Eqs. (9), (10), and (33),

$$V_{AS} = \alpha V_B. \tag{46}$$

4) Calculate the tuning ratio h from

$$h = f_B / f_{SB}. \tag{47}$$

5) Remove the driver from the enclosure, measure the driver parameters f_S, Q_{MS}, and Q_{ES} by the method of [12, Appendix],[3] and correct the driver Q values if necessary to correspond to the driver resonance frequency in the enclosure. This is done by multiplying the measured values of Q_{MS} and Q_{ES} by the ratio f_S/f_{SB}, where f_S is the resonance frequency for which Q_{MS} and Q_{ES} have been measured and f_{SB} is the resonance frequency in the enclosure found from Eq. (44). Usually if the driver parameters are measured on a test baffle of suitable size, the two resonance frequencies are almost identical and the correction is not required.

6) Calculate Q_{TS} from

$$Q_{TS} = \frac{Q_{ES} Q_{MS}}{Q_{ES} + Q_{MS}}. \tag{31}$$

7) Measure the minimum system impedance magnitude $R_E + R_{BM}$ at f_M and calculate

$$r_M = \frac{R_E + R_{BM}}{R_E}. \tag{48}$$

Then, using the corrected values of Q_{ES} and Q_{MS} obtained above, determine the total enclosure loss Q_B from the relationship

$$Q_B = \frac{h}{\alpha}\left[\frac{1}{Q_{ES}(r_M - 1)} - \frac{1}{Q_{MS}}\right]. \tag{49}$$

The term $1/Q_{MS}$ can usually be neglected.

8) The accuracy of the approximation $f_B \approx f_M$ on which the above method is based may be checked by calculating the approximate error introduced by the enclosure losses. Assuming that leakage losses are dominant in effect and that f_M is the measured frequency of zero phase, the error correction factor is

$$\frac{f_B}{f_M} = \sqrt{\frac{\alpha Q_B^2 - h^2}{\alpha Q_B^2 - 1}}. \tag{50}$$

This factor is usually quite close to unity. If it is significantly different from unity, it may be used to correct the value of f_B used in the above calculations to obtain better accuracy in the calculated parameter values.

The estimation or measurement of driver large-signal parameters is discussed in [22, Sec. 6].

With values determined for all important system parameters, system performance may be determined from the relationships given in earlier sections. The system frequency response may be calculated manually or using a digital computer but is most easily obtained by introducing the system parameters to an analog circuit simulator. The design of a simple simulator suitable for this purpose will be published in the future.

8. VENT REQUIREMENTS

The vent of a vented-box system must provide the necessary small-signal enclosure resonance frequency f_B; it must also provide the maximum required large-signal volume velocity without excessive losses or generation of spurious noises.

The second requirement can be satisfied by adjusting the vent area to a value which prevents the vent air velocity from exceeding a specified limit. An experimentally determined limit which avoids excessive noise generation is about 5% of the velocity of sound, provided that the inside of the vent is smooth and that the edges are rounded off with a reasonable radius. This velocity

[2] In [32, Appendix 4] Benson shows that if a large voice-coil inductance (or crossover inductance) is present, the measured value of f_M is lower than the true value of f_B, while f_L and f_H are negligibly affected. A much better approximation to f_B is obtained by carefully blocking the vent aperture and measuring the resonance frequency f_C of the resulting closed-box system [22]. Then, from [32, eq. (A4-6)], $f_B = (f_L^2 + f_H^2 - f_C^2)^{1/2}$. Because this relationship is true, f_C can be used directly in place of f_B in Eq. (45) to determine the system compliance ratio.

[3] Again, if the driver voice-coil inductance is large, Benson [32, Appendix 2] shows that the accuracy of determination of the Q values is improved if f_S in [12, eq. (17)] is replaced by the expression $\sqrt{f_1 f_2}$.

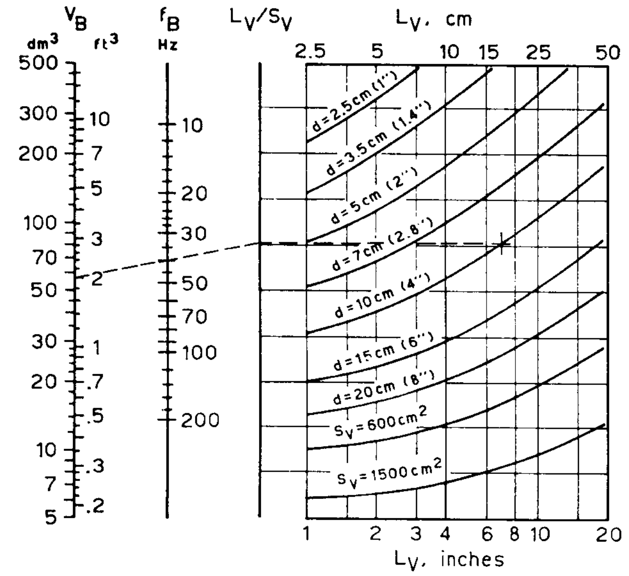

Fig. 21. Nomogram and chart for design of ducted vents.

limitation generally ensures acceptable losses as well, provided that the vent is not unduly obstructed.

The alignment, response, and power rating data of this paper combine to yield a relationship between vent area and maximum vent velocity for any given system. For program power ratings this relationship reduces to a simple approximate formula for vent area which limits the peak vent velocity, at maximum rated power input and at the frequency of maximum vent velocity, to 4½% of the velocity of sound. This formula, which is accurate within ±10% for the entire C4–B4–QB3 range of alignments, is

$$S_V \geqq 0.8 f_B V_D \tag{51}$$

or

$$d_V \geqq (f_B V_D)^{1/2} \tag{52}$$

where S_V is the area of the vent in m² or d_V is the diameter of a circular vent in meters; V_D must be expressed in m³ and f_B in Hz. Because the noise generated depends on factors other than velocity (e.g., edge roughness), and because the annoyance caused by vent noise is subjective, this formula should be regarded as a general guide only, not as a rigid rule.

Once the area of the vent is determined, the length must be adjusted to satisfy the first requirement, i.e., correct enclosure tuning. There are many popular formulas and nomograms for doing this. Using Thiele's formulas [10, eqs. (60)–(65)], the nomogram and chart of Fig. 21 were constructed to simplify the calculation process for ducted vents.

To use Fig. 21, lay a straight-edge through the enclosure volume on the V_B line and the desired resonance frequency on the f_B line and find the intersection with the L_V/S_V line. This is illustrated on the figure with lightly dashed lines for V_B = 57 dm³ (2 ft³) and f_B = 40 Hz. Next, move horizontally to the right from this intersection point until a curve is reached on the chart which corresponds to the required minimum size determined from Eqs. (51) or (52). The intersection of the horizontal projection with this curve indicates on the horizontal scale the required duct length L_V for a vent of the prescribed size. For the example illustrated, if the minimum duct diameter is 100 mm (4 inches), the required length is about 175 mm (7 inches). End corrections for one open end and one flanged end are included in the construction of the chart. For intermediate vent areas the chart may be interpolated graphically.

For some proposed systems a satisfactory vent design cannot be found. This is particularly the case for small enclosures when a low value of f_B is desired. Also, tubular vents for which the length is much greater than the diameter tend to act as half-wave resonant pipes, and any noise generated at the edge is selectively amplified. In these cases it is better to use a drone cone or passive radiator in place of the vent [2], [23]. Systems of this type will be discussed in a later paper.

9. DIAPHRAGM-VENT MUTUAL COUPLING

Mutual Coupling Magnitude

The acoustical analogous circuit of a lossless vented-box system, modified to include mutual coupling [2], [6], is presented in Fig. 22. The mutual coupling components are inside the dashed lines. (The mutual coupling resistance [2] is equal to the radiation load resistance and is therefore neglected [4], [12].)

The acoustic mutual coupling mass M_{AM} has a maximum magnitude when the diaphragm–vent spacing is a minimum. A practical minimum spacing between the centers of diaphragm and vent is about $1.5a$, where a is the diaphragm radius. Using this value, and assuming radiation conditions of a 2π-steradian free field, the maximum value of M_{AM} is about $0.13/a$ [2]. This value is reduced for a 4π-steradian free-field load [6].

For a 12-inch driver with an effective diaphragm radius of 0.12 m, the mechanical equivalent M_{MM} of the acoustic mass M_{AM} has a maximum value of 2.2g. The mechanical diaphragm mass M_{MD} for 12-inch drivers varies from about 20g for older types used in large enclosures to more than 100g for newer types designed for use in compact enclosures. Thus the mutual coupling mass may have a magnitude of from 2 to 8% of the total moving mass of the driver when all of the diaphragm air-load mass is accounted for [3, pp. 216-217].

The effect of these values of mutual coupling mass was investigated using the analog circuit simulator. A "lossless" system aligned for a B4 response was compared to the same circuit with the driver and vent masses reduced by the amount of the mutual coupling

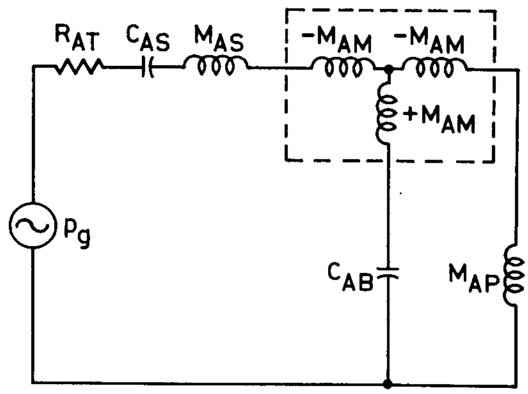

Fig. 22. Acoustical analogous circuit of lossless vented-box loudspeaker system modified to include effects of diaphragm–vent mutual coupling.

mass and the same amount of mass then introduced into the enclosure branch in agreement with Fig. 22.

Effect on Response

The effect of 2% mutual coupling mass on the frequency response could not be observed. The effect of 4% mutual coupling mass could be observed but was hardly worth taking into account. With 8% mutual coupling mass, the cutoff frequency was lowered by about 5% and the corner of the response curve became sharper as described by Locanthi. Similar effects were observed for other alignments.

It would appear that in most cases the effect of mutual coupling on system response is negligible. Only when a driver with a light diaphragm is mounted very close to the vent is the effect on response significant. It then amounts to a slight alignment shift with a very small decrease in cutoff frequency.

Effect on Measurement

Mutual coupling alters the location of the frequencies f_L and f_H of Fig. 20 but does not affect the location of f_M [2]. The shift in f_L and f_H toward each other upsets the calculation of the compliance ratio from Eq. (45), giving a value lower than the true value.

This suggests that if it is desired to measure the true compliance ratio of a system for which the magnitude of mutual coupling is very high, the vent should be blocked and the compliance ratio measured by the closed-box method described in [22]. However, if the parameters of a system are being measured only to evaluate the response of the system, the presence of mutual coupling may be ignored. Experiments on the analog circuit simulator show that the response of a system having the false calculated value of α and no mutual coupling is essentially identical to that of the actual system with its mutual coupling.

10. DISCUSSION

Features of Vented-Box Loudspeaker Systems

The vented-box loudspeaker system acts as a fourth-order high-pass filter. This basic fact determines the available range of amplitude, phase, and transient response characteristics. By suitable choice of parameters, the response may be varied from that of an extreme C4 alignment with passband ripple and very abrupt cutoff to that of an extreme QB3 alignment for which the response is effectively third order. The cost of the gentler cutoff slope and improved transient response of the QB3 alignment is a reduced value of the system efficiency factor $k_{\eta(G)}$, although this reduction is relatively small for real systems with typical enclosure losses. A further sacrifice in the value of this efficiency factor permits the use of SC4 alignments for which the transient response may approach that of a second-order system.

Perhaps the most important feature of the vented-box loudspeaker system is the very modest diaphragm excursion required at frequencies near the enclosure resonance frequency f_B. This feature is responsible for the relatively high displacement-limited power capacity of the system; it also helps to maintain low values of nonlinear distortion and modulation distortion [21].

The "misalignment" curves of Figs. 7 and 8 indicate the necessity for careful alignment of the vented-box system. The plurality of variables makes it very difficult to obtain optimum adjustment by trial-and-error methods, although simulators or computers may be used to speed up the process.

Comparison of Vented-Box and Closed-Box Systems

Most direct-radiator loudspeaker systems use or are based on either the closed-box or vented-box principle. It is therefore of interest to compare these two fundamental systems, and to observe the advantages and disadvantages of each.

One obvious difference is that the vented-box system is more complex, i.e., has more variables requiring adjustment, than the closed-box system. This difference means that satisfactory designs are relatively easier to obtain with the closed-box system and probably accounts for much of the popularity of this system.

The performance relationships derived in this paper for the vented-box system and in [22] for the closed-box system make possible a number of interesting quantitative comparisons which follow.

Response

The response of the vented-box system can typically be adjusted from fourth-order Chebyshev to quasi-third-order maximally flat; that of the closed-box system can be adjusted from second-order Chebyshev to an overdamped second-order condition approaching first-order behavior. This means the closed-box system is nominally capable of better transient response, but Thiele [10, Sec. 13] suggests the differences among correctly adjusted systems of both types are likely to be inaudible.

Efficiency

A comparison of Fig. 16 or Eq. (35) with [22, Fig. 7 or eq. (28)] reveals that the vented-box system has a maximum theoretical value of k_η which is 2.9 dB greater than that of the closed-box system. Both systems suffer to a similar degree from the combined effects of driver and enclosure losses, and both must sacrifice efficiency to make use of alignments which have better transient response than the maximum-efficiency alignment (see Fig. 15 and [22, Fig. 8]).

Typical values of k_η for practical designs still favor the vented-box system by about 3 dB. The larger efficiency constant may be used to obtain higher efficiency for the same size and cutoff frequency, a smaller enclosure size for the same efficiency and cutoff frequency, a lower cutoff frequency for the same size and efficiency, or any proportional combination of these [22, Sec. 4].

Power Capacity

The reduced diaphragm excursion of the vented-box system near the enclosure resonance frequency gives the vented-box system a higher power rating constant k_P than a comparable closed-box system. Comparing Eq. (41) with [22, eq. (35)], the advantage in favor of the vented-box system for average program material is a factor of 3.5, or 5½ dB; for particular applications it may be larger.

However, except for the extreme C4 alignments, **this** advantage is limited to the passband; at frequencies well below cutoff, the vented-box system has a higher relative displacement sensitivity and is therefore more vulnerable to turntable rumble and other subsonic signals.

Driver Requirements

For a given specification of enclosure size and system cutoff frequency, the driver of a vented-box system requires a lighter diaphragm and greater electromagnetic coupling in the magnet-voice-coil assembly compared to the same size driver used in a closed-box system (cf. example of Section 12, Part III, with that of [22, Sec. 10]). These differences are physically consistent with the higher efficiency of the vented-box system. However, for equivalent acoustic power rating, the peak displacement volume V_D and therefore the peak diaphragm displacement $x_{\max}$ is substantially smaller for the vented-box driver. Because $x_{\max}$ determines required voice-coil overhang, total amount of magnetic material required for the vented-box driver is not necessarily greater.

The closed-box system driver must have high compliance relative to the enclosure if maximum efficiency is to be achieved. While high driver compliance may be beneficial to the vented-box design in terms of transient response, it is not necessary. In fact, a maximum efficiency constant is obtained for the vented-box system with a relatively low value of compliance ratio, and maximum displacement-limited power capacity is obtained with very low values.

Enclosure Size

It is stated above that the larger value of k_η for the vented-box system may be used to obtain a size advantage, i.e., the enclosure may be smaller than that of a closed-box system having the same efficiency and cutoff frequency. Then, despite the smaller enclosure size, if the drivers have equal peak displacement volume, the larger value of k_P for the vented-box system must give a higher acoustic power rating.

This is theoretically correct, but it is practically possible only so long as V_B remains very much larger than the maximum volume displacement required. The maximum air-volume displacement from the enclosure of a vented-box system is larger than V_D because of the contribution of the vent; if this *total* volume displacement exceeds a small percentage of V_B, the compression of air within the enclosure becomes nonlinear to such a degree that the system must produce distortion regardless of the driver linearity [3, p. 274].

In most practical loudspeaker system designs, V_D is indeed very much smaller than V_B, and power capacity is not limited by enclosure size. However, if extreme miniaturization is attempted or if a driver is specifically designed to obtain a very large value of V_D, this limitation may become relevant.

It is important to realize that two direct-radiator loudspeaker systems operated at the same frequency and *acoustic* power level have the same total output volume velocity and displacement regardless of the type of system [12, eq. (2)]. Thus for both closed-box and vented-box systems, adequate enclosure volume is essential to the production of high acoustic output power with low distortion at low frequencies. Some size reduction is possible for closed-box systems if motional feedback is used to control distortion [24], but this technique can be difficult to apply successfully [25].

Typical System Performance

A sampling of commercial vented-box loudspeaker systems was tested in late 1969 by measuring the system parameters as described in Section 7 and programming these into the analog simulator to obtain the system response. For a few systems, the response obtained in this way was checked by indirect measurement [26].

Most of the samples tested fitted into the same two categories previously described for closed-box systems [22, Sec. 8]: systems with a volume of 40 dm^3 (1.5 ft^3) or more, a cutoff frequency of 50 Hz or lower, and relatively flat response; and smaller systems with a cutoff frequency above 50 Hz and several decibels of peaking in the response above cutoff. There was, however, a greater tendency for these two categories to overlap.

While most of the systems were probably designed by traditional trial-and-error methods, the general objectives of system manufacturers appear remarkably consistent. The larger systems fulfill the traditional requirements for high-fidelity reproduction, while the smaller systems suit the apparent requirements of the mass marketplace.

REFERENCES

[2] B. N. Locanthi, "Application of Electric Circuit Analogies to Loudspeaker Design Problems," *IRE Trans. Audio,* vol. PGA-6, p. 15 (Mar. 1952); republished in *J. Audio Eng. Soc.*, vol. 19, p. 778 (Oct. 1971).

[3] L. L. Beranek, *Acoustics* (McGraw-Hill, New York, 1954).

[4] F. J. van Leeuwen, "De Basreflexstraler in de Akoestiek," *Tijdschrift Nederlands Radiogenootschap,* vol. 21, p. 195 (Sept. 1956).

[6] R. H. Lyon, "On the Low-Frequency Radiation Load of a Bass-Reflex Speaker," *J. Acoust. Soc. Amer.* (Letter), vol. 29, p. 654 (May 1957).

[10] A. N. Thiele, "Loudspeakers in Vented Boxes," *Proc. IREE (Australia),* vol. 22, p. 487 (Aug. 1961); republished in *J. Audio Eng. Soc.,* vol. 19, p. 382 (May 1971), and p. 471 (June 1971).

[12] R. H. Small, "Direct-Radiator Loudspeaker System Analysis," *IEEE Trans. Audio Electroacoust.*, vol. AU-19, p. 269 (Dec. 1971); republished in *J. Audio Eng. Soc.*, vol. 20, p. 383 (June 1972).

[20] A. N. Thiele, "Equalisers for Loudspeakers," presented at the 12th National Convention of the IREE (Australia), (May 1969).

[21] P. W. Klipsch, "Modulation Distortion in Loudspeakers," *J. Audio Eng. Soc.*, vol. 17, p. 194 (Apr. 1969), and vol. 18, p. 29 (Feb. 1970).

[22] R. H. Small, "Closed-Box Loudspeaker Systems," *J. Audio Eng. Soc.*, vol. 20, p. 798 (Dec. 1972), and vol. 21, p. 11 (Jan./Feb. 1973).

[23] H. F. Olson, J. Preston, and E. G. May, "Recent Developments in Direct-Radiator High-Fidelity Loudspeakers," *J. Audio Eng. Soc.*, vol. 2, p. 219 (Oct. 1954).

[24] E. deBoer, "Theory of Motional Feedback," *IRE Trans. Audio,* vol. AU-9, p. 15 (Jan./Feb. 1961).

[25] H. W. Holdaway, "Design of Velocity-Feedback Transducer Systems for Stable Low-Frequency Behavior," *IEEE Trans. Audio,* vol. AU-11, p. 155 (Sept./Oct. 1963).

[26] R. H. Small, "Simplified Loudspeaker Measurements at Low Frequencies," *Proc. IREE (Australia),* vol. 32, p. 299 (Aug. 1971); republished in *J. Audio Eng. Soc.*, vol. 20, p. 28 (Jan./Feb. 1972).

[32] J. E. Benson, "Theory and Design of Loudspeaker Enclosures, Part 3—Introduction to Synthesis of Vented Systems," *A.W.A. Tech. Rev.*, vol. 14, p. 369 (Nov. 1972).

Vented-Box Loudspeaker Systems Part III: Synthesis

RICHARD H. SMALL

School of Electrical Engineering, The University of Sydney, Sydney, N.S.W. 2006, Australia

The analytical relationships developed in Parts I and II which relate the performance characteristics of the vented-box loudspeaker system to the basic parameters of its components make possible the straightforward design of loudspeaker systems meeting specific performance goals. A set of desired system performance specifications may be checked for realizability and then used to determine the required physical properties of all the system components. The most suitable enclosure design for a particular driver may also be readily determined.

Editor's Note: Part I of Vented-Box Loudspeaker Systems appeared in the June issue and Part II in July/August.

11. SYSTEM SYNTHESIS

System-Component Relationships

The relationships between response and system parameter adjustment are given in Part I by Figs. 6 and 9–13 for the "flat" C4–B4–QB3 alignments. Enclosure losses cannot be known exactly in advance but can be predicted from experience. For example, for numerous commercial systems and laboratory enclosures in the range of 25–100 dm³ (1–4 ft³) measured in the course of this research, the most commonly measured values of Q_B are between 5 and 10 with a general tendency for Q_B to fall with increasing enclosure volume.

For enclosures of moderate size, the assumption of an equivalent Q_L value of 7 is a very satisfactory starting point for design purposes. In this case Fig. 11 is used to represent the basic relationships between driver parameters, system parameters, and system response. If a higher or lower value of Q_B is expected with some confidence, one of the other figures is used.

The appropriate alignment and response relationships (Fig. 11 or otherwise) and the efficiency, power capacity, and vent design relationships established in Parts I and II permit the design of vented-box systems in complete detail. Procedures are described and illustrated below for two important cases, design of an enclosure to suit a particular driver and design of a complete system starting from required performance specifications.

Design with a Given Driver

The design of an enclosure to suit a given driver

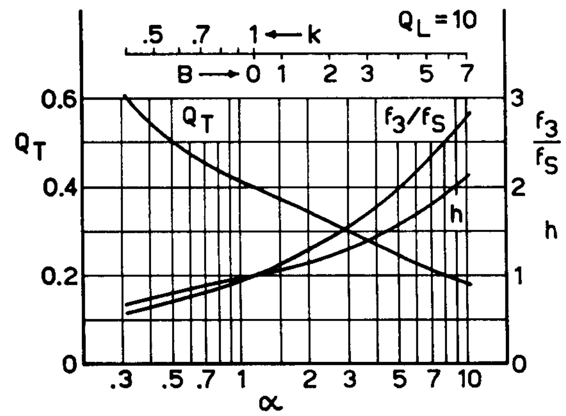

Fig. 10. Alignment chart for vented-box systems with $Q_B = Q_L = 10$.

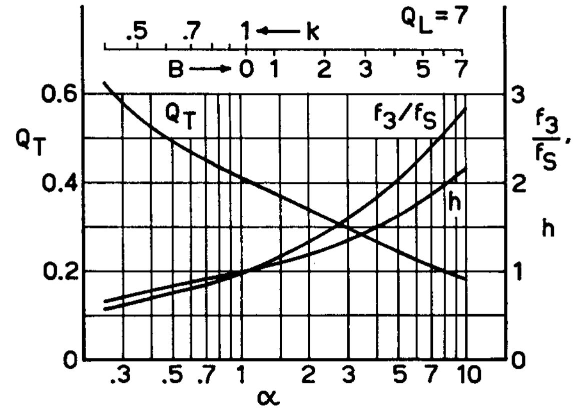

Fig. 11. Alignment chart for vented-box systems with $Q_B = Q_L = 7$.

starts with a knowledge of the driver small-signal parameters f_S, Q_{TS}, and V_{AS}; f_S and Q_{TS} must be adjusted if necessary to correspond to enclosure mounting conditions. If these parameters are not already known, they may be measured by the methods given in [10] or [12] using a standard baffle to provide air-mass loading as for an enclosure (see also Section 7 in Part II of the present paper, including Footnote 3).

The value of Q_{TS} is of primary importance. If the loudspeaker system is to be used with a modern amplifier having very low output (Thevenin) resistance, then Q_T for the system will be equal to Q_{TS} for the driver. From Figs. 6 and 9–13 it is clear that Q_T must be no larger than about 0.6 for successful application in a vented enclosure.

If Q_{TS} has a reasonable value, then the optimum value of α for a system using the driver is found from, say, Fig. 11 by locating the measured value of Q_{TS} on the Q_T curve in the figure and observing the corresponding value of α on the abscissa. This value of α then determines the optimum value of V_B using Eq. (46). It also determines the required value of h (and therefore f_B) and the corresponding value of f_3 for the system as indicated on the same figure. If the resulting system design is not acceptable (f_3 too high, V_B too large, etc.), then it is probable that the driver is not suitable for use in a vented-box system.

The design process may alternatively be begun by selecting an enclosure size V_B which suits aesthetic or architectural requirements. This determines α and hence the required enclosure tuning f_B, the required value of Q_T, and the resulting cutoff frequency f_3. If the value of f_3 is not satisfactory, then the driver and the enclosure size chosen are not compatible. If f_3 is satisfactory but the required Q_T is very different from Q_{TS}, it may be possible to use the driver as discussed below.

There are limited ways of salvaging a driver having unsatisfactory parameter values. If the value of Q_{TS} is too high to fit an alignment which is otherwise desirable in terms of enclosure size and bandwidth, an acoustically resistive material such as bonded acetate fiber may be stretched over the rear of the driver frame to reduce the effective value of Q_{MS}, thus lowering Q_{TS} [17], [27]. The correct amount of resistive material is determined experimentally by remeasurement of Q_{TS} as material is added. Q_T may also be reduced by using a negative value of amplifier output resistance R_g [10, Sec. 12], [28] to produce a low value of Q_E, where [12, eq. (21)]

$$Q_E = Q_{ES}\frac{R_g + R_E}{R_E} \tag{53}$$

because in this case [12, eq. (22)]

$$Q_T = Q_E Q_{MS}/(Q_E + Q_{MS}). \tag{54}$$

Both methods reduce Q_T without changing Q_{ES}; thus the value of $k_{\eta(Q)}$ from Eq. (29), and therefore η_0 for the system, will be lower than could be achieved by altering the magnet design to reduce Q_{ES} directly.

Sometimes the value of Q_{TS} is found to be undesirably low. This may be remedied by placing a resistor in series with the voice coil to increase R_E and therefore Q_{ES} or by using a positive value of R_g to increase Q_E.

If the driver proves satisfactory and an acceptable system design is found, the system reference efficiency is calculated from the basic driver parameters using Eq. (25). The approximate displacement-limited acoustic power rating of the system is computed from Eq. (41) if V_D is known. V_D usually can be evaluated as described in [22, Sec. 6]. The approximate displacement-limited input power rating is then found by dividing the acoustic power rating by the reference efficiency as indicated by Eq. (42). The vent design is carried out in accordance with Section 8 of Part II.

Example of Design with a Given Driver

The following small-signal parameters were measured for an 8-inch wide-range driver manufactured in the United States:

$$f_S = 33\ \text{Hz}$$

$$Q_{MS} = 2.0$$

$$Q_{ES} = 0.45$$

$$V_{AS} = 57\ \text{dm}^3\ (2\ \text{ft}^3).$$

The large-signal characteristics specified by the manufacturer are as follows.

1) "Total linear excursion of one-half inch." From this, $x_{max} = 6$ mm, and, assuming a typical effective diaphragm radius of 0.08 m,

$$V_D = 120\ \text{cm}^3.$$

2) "Power capacity 25 watts program material." From this it is assumed that for program material the thermal capacity of the driver is adequate for operation with amplifiers of up to 25-watt continuous rating.

By calculation from Eqs. (31) and (25).

$$Q_{TS} = 0.37$$
$$\eta_0 = 0.44\% .$$

Assuming that the amplifier to be used with the system has negligible Thevenin output resistance, Q_T for the system will be 0.37. Taking $Q_B = 7$ initially, Fig. 11 indicates that the enclosure volume will be relatively small; a more likely value of Q_B is thus about 10. Using Fig. 10 then, a QB3 response with $B = 1.0$ can be obtained for which the system parameters are

$$\alpha = 1.55$$
$$h = 1.07$$
$$f_3/f_S = 1.16.$$

Thus the required enclosure volume is

$$V_B = V_{AS}/\alpha = 37 \text{ dm}^3 \text{ (1.3 ft}^3\text{)}.$$

The enclosure must be tuned to

$$f_B = hf_S = 35 \text{ Hz}$$

and the system cutoff frequency is

$$f_3 = 38 \text{ Hz}.$$

From Eq. (41) the displacement-limited program acoustic power rating of the system is

$$P_{AR} = 3.0\, f_3{}^4\, V_D{}^2 = 90 \text{ mW}.$$

The corresponding displacement-limited program input power rating is

$$P_{ER} = P_{AR}/\eta_0 = 20 \text{ W}.$$

Because this is less than the manufacturer's input power rating, it should be quite safe to operate the system with an amplifier having a continuous power rating of 20 watts.

From Eq. (52) the minimum diameter of a tubular vent is $(V_D f_B)^{1/2}$ or 65 mm (2.6 inches). From Fig. 21, the required vent length is 175 mm (7 inches) for a tubing of this diameter.

Design from Specfications

The important performance specifications of a loudspeaker system include frequency response, efficiency, power capacity, and enclosure size. The complexity of the vented-box system makes control of all these specifications quite difficult when traditional trial-and-error design techniques are used. In contrast, the analytical relationships developed in this paper make possible the direct synthesis of a vented-box system to meet any physically realizable set of small-signal and large-signal specifications and even provide a check on realizability before design is begun.[4]

Specification of system frequency response basically amounts to specification of an alignment type and a cutoff frequency f_3. While the emphasis in this paper is

[4] See [32, Sec. 5 and 6] for an extensive discussion of the principles of system small-signal response synthesis.

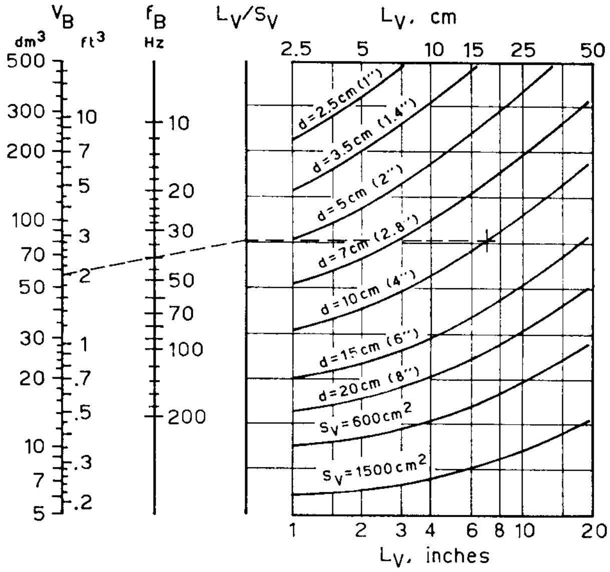

Fig. 21. Nomogram and chart for design of ducted vents.

on the "flat" C4–B4–QB3 alignments, any other desired alignment may be specified, e.g., the degenerated Chebyshev type 2 (DT2) alignment used by Nomura which provides passband peaking [11]. Appendix 1 shows how the required system alignment parameters may be calculated from the polynomial coefficients of any desired alignment based on the assumed or expected value of Q_B. For any alignment in the C4–B4–QB3 range, the necessary alignment data are provided in Figs. 9–13. The frequency response specification thus fixes the values of the parameters α, Q_T, f_S, and f_B.

For a specified frequency response, the designer may specify also the enclosure size or the reference efficiency; but he may not specify both unless the values satisfy the realizability requirements of Section 4. If the enclosure volume V_B is specified, the required driver compliance is then

$$V_{AS} = \alpha V_B. \tag{46}$$

The required value of the driver parameter Q_{ES} is found from the required value of Q_T by allowing for reasonable values of R_g (typically zero) and Q_{MS} (typically 5, but varies greatly depending on the amount of mechanical damping deliberately added to the suspension to suppress higher frequency resonances). The system efficiency is then calculated from Eq. (25).

The power capacity of the system may be specified in terms of either P_{ER} or P_{AR}, but not both unless the values agree with the attainable system efficiency. It is possible to specify both independently only if neither V_B nor η_0 are separately specified; then the required value of η_0 is given by the ratio of P_{AR} to P_{ER}, and the required enclosure volume which will provide this efficiency for the specified frequency response is found from Eqs. (26) and (28) using values of $k_{\eta(Q)}$ and $k_{\eta(G)}$ obtained from Eq. (32) and Fig. 15 and based on the estimated or expected values of Q_{MS} and Q_B.

Assuming that V_B and P_{AR} are specified and that η_0 has been determined from Eq. (25), P_{ER} is given by

$$P_{ER} = P_{AR}/\eta_0. \tag{42}$$

The required value of V_D for the driver is found from

Eq. (41) using the given values of f_3 and P_{AR}. Check that $V_D << V_B$. The thermally limited maximum input power rating of the driver $P_{E(\max)}$ must be not less than the value of P_{ER} divided by the peak-to-average power ratio of the program material to be reproduced.

The vent is designed so that the area S_V satisfies Eq. (51) and the effective length-to-area ratio gives the required f_B in combination with the enclosure volume V_B as determined from Fig. 21.

The driver is completely specified by the parameters calculated above and may be designed by the method given in Section 12.

Example of System Design from Specifications

A loudspeaker system to be used with an amplifier having very low output resistance must meet the following specifications:

$$f_3 = 40 \text{ Hz}$$
$$\text{Response} = \text{B4}$$
$$V_B = 57 \text{ dm}^3 \ (2 \text{ ft}^3)$$
$$P_{AR} = 0.25 \text{ W program peaks; expected peak-to-average power ratio 5 dB.}$$

It is assumed that the enclosure losses will correspond to $Q_B = Q_L = 7$ and that the driver mechanical losses will correspond to $Q_{MS} = 5$.

Using Fig. 11, the B4 response is located at a compliance ratio of

$$\alpha = 1.06$$

for which the required system parameters are

$$h = 1.00$$
$$f_3/f_S = 1.00$$
$$Q_T = 0.40.$$

Therefore the required driver parameters are

$$V_{AS} = 60 \text{ dm}^3 \ (2.1 \text{ ft}^3)$$
$$f_S = 40 \text{ Hz}$$
$$Q_{TS} = 0.40$$

and the required enclosure tuning is

$$f_B = 40 \text{ Hz}.$$

Taking $Q_{MS} = 5$ and using Eq. (31),

$$Q_{ES} = 0.44.$$

From Eq. (25) the reference efficiency of the system is then

$$\eta_0 = 0.84\%$$

and from Eq. (42) the displacement-limited electrical power rating is

$$P_{ER} = 30 \text{ W}.$$

This requires that the system amplifier have a continuous power rating of at least 30 watts. For the 5-dB expected peak-to-average power ratio of the program material, the thermal rating $P_{E(\max)}$ of the driver must be at least 9.5 watts [22, Sec. 5].

From Eq. (41), the displacement volume of the driver must be

$$V_D = 180 \text{ cm}^3.$$

This is only about 0.3% of V_B. Then, from Eq. (52), a tubular vent should be at least 85 mm (3.4 inches) in diameter. From Fig. 21, the length should be 115 mm (4.5 inches) for a tubing of this diameter.

12. DRIVER DESIGN

Driver Specification

The process of system design leads to specification of the required driver in terms of the basic design parameters f_S, Q_{ES}, V_{AS}, V_D, and $P_{E(\max)}$. To complete the physical specification of the driver, the arbitrary physical parameters S_D and R_E must be selected and the resulting mechanical parameters calculated. This process is described in [22, Sec. 10] and is illustrated by the example below.

Example of Driver Design

The basic design parameters of the driver required for the system in the example of the previous section are

$$f_S = 40 \text{ Hz}$$
$$Q_{ES} = 0.44$$
$$V_{AS} = 60 \text{ dm}^3$$
$$V_D = 180 \text{ cm}^3$$
$$P_{E(\max)} = 9.5 \text{ W}.$$

These specifications could be met by drivers of 8–15-inch advertized diameter [15].

Choosing a 12-inch driver, the effective diaphragm radius a will be approximately 0.12 m, giving

$$S_D = 4.5 \times 10^{-2} \text{ m}^2$$

and

$$S_D{}^2 = 2.0 \times 10^{-3} \text{ m}^4.$$

The required mechanical compliance and mass of the driver are then [22, eqs. (61) and (62)]

$$C_{MS} = V_{AS}/(\rho_0 c^2 S_D{}^2) \quad = 2.14 \times 10^{-4} \text{ m/N}$$
$$M_{MS} = 1/[(2\pi f_S)^2 C_{MS}] = 74 \text{ g}.$$

M_{MS} is the total moving mass including air loads. Assuming that the driver diaphragm occupies one third of the area of the front baffle of the enclosure and using [3, pp. 216-217] to evaluate the air loads, the mass of the voice coil and diaphragm alone is

$$M_{MD} = M_{MS} - (3.15a^3 + 0.65\pi\rho_0 a^3) = 64 \text{ g}.$$

The electromechanical damping resistance must be [22, eq. (64)]

$$B^2l^2/R_E = 2\pi f_S M_{MS}/Q_{ES} = 42 \text{ N}\cdot\text{s/m}.$$

For the popular 8Ω rating impedance, R_E is usually about 6.5 Ω. The required Bl product for such a driver is then

$$Bl = 16.5 \text{ T}\cdot\text{m}.$$

For the required displacement volume of 180 cm³, the peak linear displacement of the driver must be

$$x_{\max} = V_D/S_D = 4.0 \text{ mm}.$$

This is approximately the amount of voice-coil overhang required at each end of the magnetic gap. The total "throw" of the driver is then 8.0 mm (0.32 inch). This requirement presents no great difficulty so far as the design of the suspension is concerned.

The choice of a smaller driver diameter results in a lighter diaphragm and a less costly magnetic structure, but a greater peak displacement is then required, e.g., 9 mm (18-mm total throw) for an 8-inch driver.

The voice coil must be able to dissipate 9.5 watts nominal input power without damage.

13. DESIGN VERIFICATION

The suitability of a prototype driver designed in accordance with the above method may be checked by measuring the driver parameters as described in [12].

One of the driver parameters which is difficult to control in production is the mechanical compliance C_{MS}. Any shift in this compliance changes the measured values of both f_S and Q_{ES} as well as V_{AS}. Fortunately, system response is not critically sensitive to the value of C_{MS} so long as M_{MS} and B^2l^2/R_E have the correct values. Thus if the measured value of V_{AS} is not too far off its specified value, the driver will be satisfactory provided the quantities $f_S{}^2V_{AS}$ and f_S/Q_{ES}, which together indicate the effective moving mass and magnetic coupling, correspond to the same combinations of the specified parameters.

The effect of variations in C_{MS} on the response of a vented-box system is shown in Fig. 23 for a B4 alignment. The $\pm 50\%$ variation illustrated is larger than that commonly encountered. The relative effects are smaller for higher compliance ratios (i.e., QB3 alignments) and larger for lower compliance ratios (C4 alignments).[5]

The completed system may be checked by measuring its parameters as described in Section 7 and comparing these to the initial specifications. The actual system performance may also be verified by measurement in an anechoic environment or by an indirect method [26].

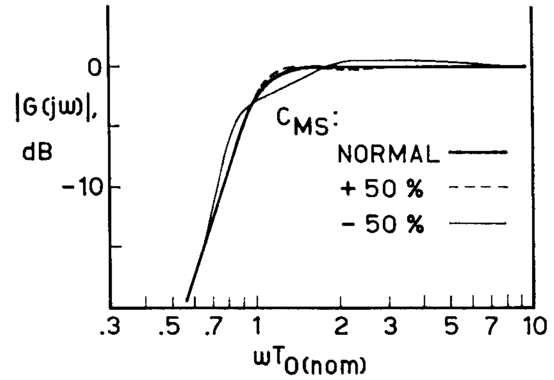

Fig. 23. Variation in frequency response of a B4-aligned vented-box system for changes in driver compliance C_{MS} of $\pm 50\%$ (from simulator).

14. SPECIFICATIONS AND RATINGS

Drivers

The moving-coil or electrodynamic driver has long been the workhorse of the loudspeaker industry. However, system designers have not been fully aware of the importance or usefulness of a knowledge of the important fundamental parameters of these drivers. They have instead used trial-and-error design techniques and relied on acoustical measurements of a completed system to determine the performance characteristics of the system.

The most important message of this paper and those that have preceded it is that trial-and-error design techniques are not only wasteful but unnecessary. Design may be carried out by direct synthesis provided the system designer either knows the parameters of a given driver or can obtain a desired driver by specifying its parameters.

It is essential for a driver manufacturer to specify all the important parameters of a driver so that system designers can completely evaluate the small-signal and large-signal performance obtainable from that driver. In addition to the specific physical properties of diaphragm size and voice-coil resistance (or rating impedance), the designer needs to know the values of the parameters f_S, Q_{ES}, Q_{MS}, V_{AS}, V_D, and $P_{E(\max)}$. Conversely, where the designer needs a driver having particular values of these parameters, the driver manufacturer must be able to work from such specifications to produce the driver.

Because the basic design parameters above are directly related to the fundamental mechanical parameters such as M_{MD}, C_{MS}, B, and l, which the driver manufacturer has long used, there need be no difficulty in supplying these parameters. There is every likelihood that feedback from system designers will be helpful to driver manufacturers in improving their products, particularly in finding the best tradeoffs among response, efficiency, and power capacity requirements which can be obtained for a given cost.

Systems

Because the frequency response, reference efficiency, and displacement-limited power capacity of a vented-box loudspeaker system are all directly related to a relatively small number of easily measured system and driver parameters, there is every incentive for system manufacturers to provide complete data on these fundamental performance characteristics with the basic system specifications.

The theoretical relationships developed here refer to a standard radiation load of a 2π-steradian free field. This is only an approximation to average listening-room conditions [29], but ratings and specifications based on these relationships are of unquestionable value in comparing the expected performance of different systems in a particular application.

There is little doubt that buyers and users of loudspeaker systems would appreciate an increase in the amount of quantitative and directly comparable data supplied with such systems, especially in the categories of reference efficiency and acoustic power capacity.

15. CONCLUSION

The vented-box loudspeaker system has been popular for decades but has recently been shunned in favor of the more easily designed closed-box system.

The quantitative relationships presented in this paper make the design of vented-box systems a relatively simple task, despite the complexity of these systems.

[5] A very recent paper by Keele [33] contains exact calculations of the sensitivity factors of vented-box alignments to all important driver and system parameters. The sensitivity to driver compliance is shown to be extremely low compared to that for most other parameters over a wide range of alignments.

They also indicate that the vented-box system has substantial advantages over the closed-box system in terms of the attainable values of the efficiency and power-rating constants, although these advantages are gained at the expense of transient response and immunity to subsonic signals.

As the design of vented-box systems becomes better understood, interest in these systems may be expected to increase again. This does not mean that the popularity of well-designed closed-box systems will diminish. The choice of one or the other will depend on the requirements of a particular application.

The ease with which the low-frequency performance of a loudspeaker system may be specified in terms of simply measured system parameters should encourage more complete specification by manufacturers of the important frequency response, reference efficiency, and power capacity characteristics of their products.

16. ACKNOWLEDGMENT

This paper is part of the result of a program of postgraduate research into the low-frequency performance of direct-radiator electrodynamic loudspeaker systems. I am indebted to the School of Electrical Engineering of the University of Sydney for providing research facilities, supervision, and assistance, and to the Australian Commonwealth Department of Education and Science for financial support.

My indebtedness to A. N. Thiele for the inspiration behind the research program has already been acknowledged. We are also grateful for his considerable encouragement, helpful suggestions, and valuable criticisms of techniques and results.

I am further indebted to J. E. Benson for his generous assistance in discussing the subject matter of this paper and in examining and criticizing early manuscripts, and to Dr. R. H. Frater for his valuable contributions to the organization of this paper.

Finally, I acknowledge with gratitude the generous and considerable efforts of R. C. Pols in providing an English translation of the van Leeuwen paper.

REFERENCES

[3] L. L. Beranek, *Acoustics* (McGraw-Hill, New York, 1954).

[10] A. N. Thiele, "Loudspeakers in Vented Boxes," *Proc. IREE (Australia)*, vol. 22, p. 487 (Aug. 1961); republished in *J. Audio Eng. Soc.*, vol. 19, p. 382 (May 1971), and p. 471 (June 1971).

[11] Y. Nomura, "An Analysis of Design Conditions of a Bass-Reflex Loudspeaker Enclosure for Flat Response," *Electron. Commun. Japan*, vol. 52-A, no. 10, p. 1 (1969).

[12] R. H. Small, "Direct-Radiator Loudspeaker System Analysis," *IEEE Trans. Audio Electroacoust.*, vol. AU-19, p. 269 (Dec. 1971); republished in *J. Audio Eng. Soc.*, vol. 20, p. 383 (June 1972).

[15] J. R. Ashley and M. D. Swan, "Improved Measurement of Loudspeaker Driver Parameters," presented at the 40th Convention of the Audio Engineering Society, Los Angeles (Apr. 1971). Preprint 803.

[17] J. F. Novak, "Designing a Ducted-Port Bass-Reflex Enclosure," *Electron. World*, vol. 75, p. 25 (Jan. 1966).

[22] R. H. Small, "Closed-Box Loudspeaker Systems," *J. Audio Eng. Soc.*, vol. 20, p. 798 (Dec. 1972); vol. 21, p. 11 (Jan./Feb. 1973).

[26] R. H. Small, "Simplified Loudspeaker Measurements at Low Frequencies," *Proc. IREE (Australia)*, vol. 32, p. 299 (Aug. 1971); republished in *J. Audio Eng. Soc.*, vol. 20, p. 28 (Jan./Feb. 1972).

[27] J. L. Grauer, "Acoustic Resistance Damping for Loudspeakers," *Audio*, vol. 49, p. 22 (Mar. 1965).

[28] W. Steiger, "Transistor Power Amplifiers with Negative Output Impedance," *IRE Trans. Audio*, vol. AU-8, p. 195 (Nov./Dec. 1960).

[29] R. F. Allison and R. Berkovitz, "The Sound Field in Home Listening Rooms," *J. Audio Eng. Soc.*, vol. 20, p. 459 (July/Aug. 1972).

[32] J. E. Benson, "Theory and Design of Loudspeaker Enclosures, Part 3—Introduction to Synthesis of Vented Systems," *A.W.A. Tech. Rev.*, vol. 14, p. 369 (Nov. 1972).

[33] D. B. Keele, Jr., "Sensitivity of Thiele's Vented Loudspeaker Enclosure Alignments to Parameter Variations," *J. Audio Eng. Soc.*, vol. 21, p. 246 (May 1973).

Vented-Box Loudspeaker Systems Part IV: Appendices

RICHARD H. SMALL

School of Electrical Engineering, The University of Sydney, Sydney, N.S.W. 2006, Australia

The appendices present a method of calculating the system parameters required to obtain a desired alignment defined by transfer-function polynomial coefficients in the presence of enclosure losses together with diaphragm displacement data for that alignment, a derivation of the parameter-impedance relationships that permit parameter evaluation from voice-coil impedance measurements, and a method of evaluating the amounts of absorption, leakage, and vent losses present in a vented-box loudspeaker system.

Editor's Note: Part I of Vented-Box Loudspeaker Systems appeared in the June issue, Part II in July/August, and Part III in September.

APPENDIX 1 FOURTH-ORDER FILTER FUNCTIONS AND VENTED-BOX SYSTEM ALIGNMENT

General Expressions

The general form of a prototype low-pass fourth-order filter function $G_L(s)$ normalized to unity in the passband is

$$G_L(s) = \frac{1}{1 + a_1 sT_0 + a_2 s^2 T_0^2 + a_3 s^3 T_0^3 + s^4 T_0^4} \quad (55)$$

where T_0 is the nominal filter time constant and the coefficients a_1, a_2, and a_3 determine the actual filter characteristic.

Tables of filter functions normally give only the details of a low-pass prototype function; the high-pass and bandpass equivalents are obtained by suitable transformation. For the high-pass filter function $G_H(s)$, the transformation (retaining the same nominal time constant) is

$$G_H(sT_0) = G_L(1/sT_0). \quad (56)$$

This leads to the general high-pass form of Eq. (20):

$$G_H(s) = \frac{s^4 T_0^4}{s^4 T_0^4 + a_1 s^3 T_0^3 + a_2 s^2 T_0^2 + a_3 s T_0 + 1}. \quad (57)$$

Study of the magnitude-versus-frequency behavior of filter functions is facilitated by the use of the magnitude-squared form

$$|G_H(j\omega)|^2 = \frac{\omega^8 T_0^8}{\omega^8 T_0^8 + A_1 \omega^6 T_0^6 + A_2 \omega^4 T_0^4 + A_3 \omega^2 T_0^2 + 1} \quad (58)$$

where

$$\begin{aligned} A_1 &= a_1^2 - 2a_2 \\ A_2 &= a_2^2 + 2 - 2a_1 a_3 \\ A_3 &= a_3^2 - 2a_2. \end{aligned} \quad (59)$$

Using Eq. (58) it can be shown that the magnitude response of G_H is down 3 dB, i.e., $|G_H|^2 = 1/2$, at a frequency f_3 given by

$$f_3/f_0 = d^{1/2} \quad (60)$$

where

$$f_0 = 1/(2\pi T_0) \quad (61)$$

and d is the largest positive real root of the equation

$$d^4 - A_1 d^3 - A_2 d^2 - A_3 d - 1 = 0. \quad (62)$$

Coefficients of Some Useful Responses

Butterworth Maximally Flat Amplitude Response (B4)

This well-known response is characterized by [10], [18]

$$a_1 = (4+2\sqrt{2})^{1/2} = 2.6131$$
$$a_2 = 2+\sqrt{2} = 3.1412$$
$$a_3 = a_1 = 2.6131$$
$$A_1 = A_2 = A_3 = 0$$
$$f_3/f_0 = 1.0000$$

Bessel Maximally Flat Delay Response (BL4)

The normalized roots are given in [19]. They yield

$$a_1 = 3.20108 \quad A_1 = 1.4638$$
$$a_2 = 4.39155 \quad A_2 = 1.2857$$
$$a_3 = 3.12394 \quad A_3 = 0.9759.$$
$$f_3/f_0 = 1.5143$$

Chebyshev Equal-Ripple (C4) and "Sub-Chebyshev" (SC4) Responses

These responses are both described in [14]; the $C4$ responses are further described in [32]. The pole locations may be derived from those of the Butterworth response by multiplying the real part of the Butterworth pole by a factor k which is less than unity for the $C4$ responses and greater than unity for the $SC4$ responses. The filter-function coefficients are then given by

$$a_3 = \frac{k(4+2\sqrt{2})^{1/2}}{D^{1/4}}$$
$$a_2 = \frac{1+k^2(1+\sqrt{2})}{D^{1/2}}$$
$$a_1 = \frac{a_3}{D^{1/2}}\left[1-\frac{1-k^2}{2\sqrt{2}}\right] \tag{63}$$

where

$$D = \frac{k^4+6k^2+1}{8}.$$

For the $C4$ responses, the passband ripple is given by

$$\text{dB ripple} = 10\log_{10}[1+K^4/(64+28K+80K^2+16K^3)] \tag{64}$$

where

$$K = 1/k^2 - 1.$$

Quasi-Third-Order Butterworth Responses (QB3)

This class of response is described in [10] and [32]. In this paper, the response is varied as a function of the parameter B given by

$$B = A_3^{1/2}. \tag{65}$$

The other coefficients are given by

$$A_1 = A_2 = 0$$
$$a_2 > 2+\sqrt{2}$$
$$a_1 = (2a_2)^{1/2}$$
$$a_3 = (a_2^2+2)/(2a_1). \tag{66}$$

Because the direct relationships between B and the a coefficients are very involved, the range of responses is computed by taking successive values of a_2 and then computing a_1, a_3, A_3, and B.

Other Possible Responses

Other fourth-order responses which can be obtained with the vented-box system include transitional Butterworth–Thompson [18], transitional Butterworth–Chebyshev [30], Thiele interorder [31], and degenerated Chebyshev [11].

The degenerated Chebyshev responses of the second kind ($DT2$) described by Nomura [11] look particularly appealing for cases where a smooth bass lift (similar to an underdamped second-order response, but with a steeper cutoff slope) is desired. Nomura's design parameters are readily convertible into those of this paper.

Computation of Basic Alignment Data

The basic alignment data are obtained by using the coefficient–parameter relationships given by Eqs. (21)–(24). The steps are as follows.

1) For a given response and value of Q_L calculate

$$c_1 = a_1Q_L$$
$$c_2 = a_3Q_L. \tag{67}$$

2) Find the positive real root r of

$$r^4 - c_1r^3 + c_2r - 1 = 0. \tag{68}$$

3) Then, using Eqs. 60–62 to obtain f_3/f_0, the alignment parameters are

$$h = r^2$$
$$f_3/f_S = h^{1/2}(f_3/f_0)$$
$$\alpha = a_2h - h^2 - 1 - (1/Q_L^2)(a_3h^{1/2}Q_L - 1)$$
$$Q_T = hQ_L/(a_3h^{1/2}Q_L - 1). \tag{69}$$

For infinite Q_L the above expressions reduce to Thiele's formulas:

$$h = a_3/a_1$$
$$f_3/f_S = h^{1/2}(f_3/f_0)$$
$$\alpha = a_2h - h^2 - 1$$
$$Q_T = 1/(a_1a_3)^{1/2}. \tag{70}$$

Computation of Displacement Maxima

Eq. (14) may be written in the generalized form

$$X(s) = \frac{b_1s^2T_0^2 + b_2sT_0 + 1}{s^4T_0^4 + a_1s^3T_0^3 + a_2s^2T_0^2 + a_3sT_0 + 1} \tag{71}$$

where T_0, a_1, a_2, and a_3 are given by Eqs. (21)–(24) or by the alignment specification and

$$b_1 = 1/h$$
$$b_2 = 1/(h^{1/2}Q_L). \tag{72}$$

The magnitude-squared form of this expression is

$$|X(j\omega)|^2 = \frac{B_1\omega^4T_0^4 + B_2\omega^2T_0^2 + 1}{\omega^8T_0^8 + A_1\omega^6T_0^6 + A_2\omega^4T_0^4 + A_3\omega^2T_0^2 + 1} \tag{73}$$

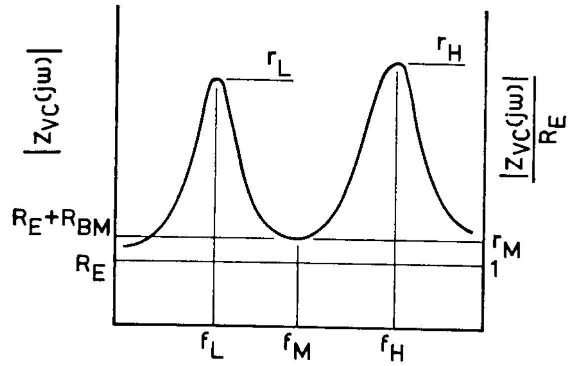

Fig. 20. Voice-coil impedance magnitude of vented-box loudspeaker system as a function of frequency.

where the A_i coefficients are given by Eq. (59) and

$$B_1 = b_1^2$$
$$B_2 = b_2^2 - 2b_1. \tag{74}$$

The value of $|X(j\omega)|_{\max}^2$ for any alignment is found by differentiating Eq. (73), setting the result equal to zero, solving for the value of $\omega^2 T_0^2$, and then replacing this solution in Eq. (73) and evaluating the expression. There are always at least three frequencies of zero slope for Eq. (73): zero, near f_B, and above f_B. For the extreme $C4$ alignments, there is a fourth frequency, below f_B. The first of these frequencies gives unity displacement; the second is not of interest because it gives a displacement minimum. The third frequency gives the displacement needed to evaluate the displacement-limited power capacity for bandwidth-limited drive conditions. The procedure is as follows.

1) For a given alignment and value of Q_L, calculate

$$\begin{aligned} C_4 &= (1/2B_1)(A_1B_1 + 3B_2) \\ C_3 &= (1/B_1)(A_1B_2 + 2) \\ C_2 &= (1/2B_1)(3A_1 + A_2B_2 - A_3B_1) \\ C_1 &= (1/B_1)(A_2 - B_1) \\ C_0 &= (1/2B_1)(A_3 - B_2). \end{aligned} \tag{75}$$

2) Find the largest positive real root G of

$$G^5 + C_4G^4 + C_3G^3 + C_2G^2 + C_1G + C_0 = 0. \tag{76}$$

(The normalized frequency of maximum passband displacement is then $f_{X\max}/f_0 = G^{1/2}$).

3) Calculate

$$|X(j\omega)|_{\max}^2 = \frac{B_1G^2 + B_2G + 1}{G^4 + A_1G^3 + A_2G^2 + A_3G + 1}. \tag{77}$$

The same procedure is used to determine the frequency of maximum displacement below f_B for the extreme $C4$ alignments by finding the smallest nonzero positive real root in 2). The corresponding maximum value of the displacement function magnitude is then determined as in 3).

APPENDIX 2 PARAMETER-IMPEDANCE RELATIONSHIPS

Determination of f_{SB} and α

For infinite Q_L, the steady-state form of Eq. (16) becomes

$$Z_{VC}(j\omega) = R_E + R_{ES}\frac{j(\omega T_S/Q_{MS})(1-\omega^2T_B^2)}{\omega^4T_B^2T_S^2 + 1 + \omega^2[(\alpha+1)T_B^2 + T_S^2] + j(\omega T_S/Q_{MS})(1-\omega^2T_B^2)}. \tag{78}$$

This expression has minimum magnitude and zero phase when the numerator of the second term is zero, i.e., when $\omega = 1/T_B$. Thus for this case, the frequency f_M of Fig. 20 is equal to f_B. The expression also has zero phase, with maximum magnitude, when the real part of the denominator of the second term is zero, i.e., for

$$\omega^2 = \frac{T_S^2 + (\alpha+1)T_B^2 \pm \sqrt{T_S^4 + (\alpha+1)^2T_B^4 + (2\alpha-2)T_B^2T_S^2}}{2T_B^2T_S^2}. \tag{79}$$

Let the solution using the plus sign be ω_H^2 and the solution using the minus sign be ω_L^2. Then

$$\omega_H^2 + \omega_L^2 = \omega_B^2 + (\alpha+1)\omega_S^2 \tag{80}$$

and

$$(\omega_H^2 - \omega_L^2)^2 = \omega_B^4 + (\alpha+1)^2\omega_S^4 + (2\alpha-2)\omega_B^2\omega_S^2. \tag{81}$$

Combining Eqs. (80) and (81), it can be shown that

$$(\omega_H^2 - \omega_L^2)^2 = (\omega_H^2 + \omega_L^2)^2 - 4\omega_B^2\omega_S^2 \tag{82}$$

which simplifies to

$$\omega_H^2\omega_L^2 = \omega_S^2\omega_B^2$$

or [10, eq. (105)]

$$f_S = \frac{f_Hf_L}{f_B} \tag{83}$$

where $f_S = f_{SB}$ is the resonance frequency of the driver for the particular air-load mass presented by the enclosure.

With f_S known, α can be found by rearranging Eq. (80) into

$$\alpha = \frac{f_H^2 + f_L^2 - f_B^2}{f_S^2} - 1. \tag{84}$$

Alternatively, substituting Eq. (83) into Eq. (80), it is easily shown that [10, eq. (106)]

$$\alpha = \frac{(f_H^2 - f_B^2)(f_B^2 - f_L^2)}{f_H^2f_L^2}. \tag{85}$$

This expression factors into

$$\alpha = \frac{(f_H + f_B)(f_H - f_B)(f_B + f_L)(f_B - f_L)}{f_H^2f_L^2}. \tag{45}$$

Approximate Determination of Q_B

From Fig. 3, Z_{VC} will be resistive when the portion of the circuit to the right of R_{ES} is resistive. The steady-state impedance of this portion of the circuit is

$$Z(j\omega) = R_{EL}\frac{(\alpha T_BQ_L)[-\omega^2T_B/Q_L + j\omega(1-\omega^2T_B^2)]}{\omega^4T_B^2T_S^2 + 1 - \omega^2[(\alpha+1)T_B^2 + T_S^2] + j\omega(T_B/Q_L)(1-\omega^2T_S^2)} \tag{86}$$

At a frequency of zero phase, the magnitude of $Z(j\omega)$ may be evaluated by taking the ratio of either the real or the imaginary parts of the numerator and denominator, because these ratios must be equal. That is, for zero phase,

$$|Z(j\omega)| = R_{EL}(aT_BQ_L)\frac{-\omega^2T_B/Q_L}{\omega^4T_B{}^2T_S{}^2+1-\omega^2[(a+1)T_B{}^2+T_S{}^2]}$$
$$= R_{EL}(aT_BQ_L)\frac{1-\omega^2T_B{}^2}{(T_B/Q_L)(1-\omega^2T_S{}^2)}. \qquad (87)$$

Setting the real and imaginary ratios equal in the normal way leads to a very complex set of solutions for the exact frequencies of zero phase. However, it can be seen that the first ratio varies relatively slowly with frequency near ω_B (as indeed does $|Z_{VC}(j\omega)|$) and hence can be expected to have about the same magnitude at the frequency of zero phase ω_M very near to ω_B as it has at ω_B. This gives

$$|Z(j\omega_M)| \approx |Z(j\omega_B)| = R_{EL}. \qquad (88)$$

The resistive voice-coil impedance measured at f_M, defined as $R_E + R_{BM}$ in Fig. 20, is thus made up of R_E plus the parallel combination of R_{ES} and R_{EL}. Evaluating this resistance and using Eqs. (5), (7), (8), (10), and (11), it can be shown that

$$Q_L = \frac{h}{a}\left[\frac{1}{Q_{ES}(r_M-1)} - \frac{1}{Q_{MS}}\right] \qquad (49)$$

where r_M is $(R_E + R_{BM})/R_E$ as defined in Eq. (48) and Fig. 20. In many cases the $1/Q_{MS}$ term can safely be neglected.

Now, if the two ratios in Eq. (87) are equal at ω_M, the second must give the same value as the first. This requires that

$$\omega_M{}^2 = \frac{1-aQ_L{}^2}{T_S{}^2 - aT_B{}^2Q_L{}^2} \qquad (89)$$

which may be rearranged to give Eq. (50). The approximation made earlier in Eq. (88) seems justified by Eq. (50) for Q_B values as low as 5, because the difference between f_M and f_B is then at most a few percent. For lower values of Q_B (which are unusual), substantial inaccuracy must be expected. Inaccuracy can also be contributed by a significant voice-coil inductance (see [32]).

APPENDIX 3
MEASUREMENT OF ENCLOSURE LOSSES

Measurement Principle

In this method of measurement the system driver is used as a coupling transducer between the enclosure impedances and the electrical measuring equipment. The driver losses are subtracted from the total measured losses to obtain the enclosure losses. Greatest accuracy is therefore obtained where the driver mechanical losses are small and stable.

The method assumes that R_E remains constant with frequency (i.e., voice-coil inductance losses are negligible), that the individual enclosure circuit losses correspond to Q values of about 5 or more (so that $Q^2 >> 1$), and that any variation with frequency of the actual losses present can still be represented effectively by a combination of the three fixed resistances R_{AB}, R_{AL}, and R_{AP} of Fig. 1.

System Loss Data

From the system impedance curve, Fig. 20, find the three frequencies f_L, f_M, and f_H, and the ratio of the corresponding maximum or minimum impedance to R_E, designated r_L, r_M, and r_H.

Using the methods of Section 7 (Part II) or [32], determine the system compliance ratio a. Measure independently the driver resonance frequency f_S and the corresponding value of Q_{ES} as described in [12] or [32]. The driver mounting conditions for the latter measurements do not matter, because the product f_SQ_{ES} which will be used is independent of the air-load mass present.

Driver Loss Data

Let the symbol ρ be used to define the ratio

$$\rho = (R_{ES} + R_E)/R_E. \qquad (90)$$

Because R_{ES} is in fact a function of frequency for real drivers, so too is ρ. Typically the variation is of the order of 2 to 4 dB per octave increase with increasing frequency.

At the resonance frequency of the driver, ρ is the ratio of the maximum voice-coil impedance to R_E which is defined as r_0 in [12]. The value of ρ for frequencies down to f_L may be measured by weighting (mass loading) the driver diaphragm and measuring the maximum voice-coil impedance at resonance for a number of progressively lower frequencies as more and more mass is added. A convenient nondestructive method of weighting is to stick modeling clay or plasticene to the diaphragm near the voice coil.

Unfortunately, there is no comparable simple way to reduce mass or add stiffness which will raise the driver resonance frequency without affecting losses. For simplicity, it is necessary to extrapolate the low-frequency data upward to f_H. This is risky if f_H is more than an octave above f_S but gives quite reasonable results for many drivers.

Under laboratory conditions, it is possible to fabricate a low-mass driver which is "normally" operated with a fixed value of added mass. This mass is selected so that the unloaded driver resonance occurs at a frequency equal to or greater than the value of f_H for the loaded driver in a particular enclosure. In this case the value of ρ can be accurately determined for the entire required frequency range by adding and removing mass.

Measure and plot (extrapolating if necessary) the value of ρ over the frequency range f_L to f_H. Find the values at f_L, f_M, and f_H and designate these ρ_L, ρ_M, and ρ_H.

These measurements should be carried out at the same time and under the same conditions as those for the system loss data above. The signal level should be the same and should be within small-signal limits at all times.

Enclosure Loss Calculation

Define:

$$H = f_H/f_M$$
$$L = f_M/f_L$$
$$F = f_M/(af_SQ_{ES}). \qquad (91)$$

Calculate:

$$k_L = \frac{1}{r_L - 1} - \frac{1}{\rho_L - 1}$$
$$k_M = \frac{1}{r_M - 1} - \frac{1}{\rho_M - 1}$$
$$k_H = \frac{1}{r_H - 1} - \frac{1}{\rho_H - 1} \qquad (92)$$

$$C_L = Fk_L(L^2 - 1)\left(1 - \frac{1}{L^2}\right)$$
$$C_M = (Fk_M)^{-1}$$
$$C_H = Fk_H(H^2 - 1)\left(1 - \frac{1}{H^2}\right) \qquad (93)$$

$$\Delta = \left(H^2L^2 - \frac{1}{H^2L^2}\right) - \left(H^2 - \frac{1}{L^2}\right) - \left(L^2 - \frac{1}{H^2}\right)$$
$$N_L = C_M\left(H^2L^2 - \frac{1}{H^2L^2}\right) - C_H\left(L^2 - \frac{1}{L^2}\right) - C_L\left(H^2 - \frac{1}{H^2}\right)$$
$$N_A = -C_M\left(L^2 - \frac{1}{H^2}\right) + C_H(L^2 - 1) + C_L\left(1 - \frac{1}{H^2}\right)$$
$$N_P = -C_M\left(H^2 - \frac{1}{L^2}\right) + C_H\left(1 - \frac{1}{L^2}\right) + C_L(H^2 - 1). \qquad (94)$$

Then the values of Q_L, Q_A, and Q_P which apply at the frequency f_M are found from

$$Q_L = \Delta/N_L$$
$$Q_A = \Delta/N_A$$
$$Q_P = \Delta/N_P. \qquad (95)$$

Using the same data, the total enclosure loss Q_B at the frequency f_M is

$$Q_B(f_M) = 1/C_M = Fk_M. \qquad (96)$$

The approximate formula for $Q_B = Q_L$ given in Eq. (49) differs from Eq. (96) only in that R_{ES} is assumed constant, i.e., that $\rho_M = r_0$. However, because ρ_M is seldom very different from r_0, and particularly because $r_M - 1$ is usually much less than $\rho_M - 1$, Eq. (49) provides an adequately accurate measurement of total losses for normal evaluation purposes.

REFERENCES

[1] A. L. Thuras, "Sound Translating Device," U. S. Patent 1,869,178, application Aug. 15, 1930; patented July 26, 1932.

[2] B. N. Locanthi, "Application of Electric Circuit Analogies to Loudspeaker Design Problems," *IRE Trans. Audio*, vol. PGA-6, p. 15 (Mar. 1952); republished in *J. Audio Eng. Soc.*, vol. 19, p. 778 (Oct. 1971).

[3] L. L. Beranek, *Acoustics* (McGraw-Hill, New York, 1954).

[4] F. J. van Leeuwen, "De Basreflexstraler in de Akoestiek," *Tijdschrift Nederlands Radiogenootschap*, vol. 21, p. 195 (Sept. 1956).

[5] E. de Boer, "Acoustic Interaction in Vented Loudspeaker Enclosures," *J. Acoust. Soc. Amer.* (Letter), vol. 31, p. 246 (Feb. 1959).

[6] R. H. Lyon, "On the Low-Frequency Radiation Load of a Bass-Reflex Speaker," *J. Acoust. Soc. Amer.* (Letter), vol. 29, p. 654 (May 1957).

[7] J. F. Novak, "Performance of Enclosures for Low-Resonance High-Compliance Loudspeakers," *IRE Trans. Audio*, vol. AU-7, p. 5 (Jan./Feb. 1959); also *J. Audio Eng. Soc.*, vol. 7, p. 29 (Jan. 1959).

[8] L. Keibs, "The Physical Conditions for Optimum Bass Reflex Cabinets," *J. Audio Eng. Soc.*, vol. 8, p. 258 (Oct. 1960).

[9] E. de Boer, "Synthesis of Bass-Reflex Loudspeaker Enclosures," *Acustica*, vol. 11, p. 1 (1961).

[10] A. N. Thiele, "Loudspeakers in Vented Boxes," *Proc. IREE (Australia)*, vol. 22, p. 487 (Aug. 1961); republished in *J. Audio Eng. Soc.*, vol. 19, p. 382 (May 1971), and p. 471 (June 1971).

[11] Y. Nomura, "An Analysis of Design Conditions of a Bass-Reflex Loudspeaker Enclosure for Flat Response," *Electron. Commun. Japan*, vol. 52-A, no. 10, p. 1 (1969).

[12] R. H. Small, "Direct-Radiator Loudspeaker System Analysis," *IEEE Trans. Audio Electroacoust.*, vol. AU-19, p. 269 (Dec. 1971); republished in *J. Audio Eng. Soc.*, vol. 20, p. 383 (June 1972).

[13] D. E. L. Shorter, "Loudspeaker Cabinet Design," *Wireless World*, vol. 56, p. 382 (Nov. 1950), p. 436 (Dec. 1950).

[14] A. N. Thiele, "Filters with Variable Cut-off Frequencies," *Proc. IREE (Australia)*, vol. 26, p. 284 (Sept. 1965).

[15] J. R. Ashley and M. D. Swan, "Improved Measurement of Loudspeaker Driver Parameters," presented at the 40th Convention of the Audio Engineering Society, Los Angeles (Apr. 1971), Preprint 803.

[16] B. C. Reith, "Bass-Reflex Enclosures," *Wireless World* (Letter), vol. 73, p. 38 (Jan. 1967).

[17] J. F. Novak, "Designing a Ducted-Port Bass-Reflex Enclosure," *Electron. World*, vol. 75, p. 25 (Jan. 1966).

[18] L. Weinberg, *Network Analysis and Synthesis* (McGraw-Hill, New York, 1962), ch. 11.

[19] R. M. Golden and J. F. Kaiser, "Root and Delay Parameters for Normalized Bessel and Butterworth Low-Pass Transfer Functions," *IEEE Trans. Audio Electroacoust.*, vol. AU-19, p. 64 (Mar. 1971).

[20] A. N. Thiele, "Equalisers for Loudspeakers," presented at the 12th National Convention of the IREE (Australia), (May 1969).

[21] P. W. Klipsch, "Modulation Distortion in Loudspeakers," *J. Audio Eng. Soc.*, vol. 17, p. 194 (Apr. 1969), and vol. 18, p. 29 (Feb. 1970).

[22] R. H. Small, "Closed-Box Loudspeaker Systems," *J. Audio Eng. Soc.*, vol. 20, p. 798 (Dec. 1972), and vol. 21, p. 11 (Jan./Feb. 1973).

[23] H. F. Olson, J. Preston, and E. G. May, "Recent Developments in Direct-Radiator High-Fidelity Loudspeakers," *J. Audio Eng. Soc.*, vol. 2, p. 219 (Oct. 1954).

[24] E. de Boer, "Theory of Motional Feedback," *IRE Trans. Audio*, vol. AU-9, p. 15 (Jan./Feb. 1961).

[25] H. W. Holdaway, "Design of Velocity-Feedback Transducer Systems for Stable Low-Frequency Behavior," *IEEE Trans. Audio*, vol. AU-11, p. 155 (Sept./Oct. 1963).

[26] R. H. Small, "Simplified Loudspeaker Measurements at Low Frequencies," *Proc. IREE (Australia)*, vol. 32, p. 299 (Aug. 1971); republished in *J. Audio Eng. Soc.*, vol. 20, p. 28 (Jan./Feb. 1972).

[27] J. L. Grauer, "Acoustic Resistance Damping for Loudspeakers," *Audio*, vol. 49, p. 22 (Mar. 1965).

[28] W. Steiger, "Transistor Power Amplifiers with Negative Output Impedance," *IRE Trans. Audio*, vol. AU-8, p. 195 (Nov./Dec. 1960).

[29] R. F. Allison and R. Berkovitz, "The Sound Field in Home Listening Rooms," *J. Audio Eng. Soc.*, vol. 20, p. 459 (July/Aug. 1972).

[30] A. Budak and P. Aronhime, "Transitional Butterworth–Chebyshev Filters," *IEEE Trans. Circuit Theory* (Correspondence), vol. CT-18, p. 413 (May 1971).

[31] A. N. Thiele, "Response Shapes for Simplified Active Filters," *Proc. IREE (Australia)*, to be published.

[32] J. E. Benson, "Theory and Design of Loudspeaker Enclosures, Part 3—Introduction to Synthesis of Vented Systems," *A.W.A. Tech. Rev.*, vol. 14, p. 369 (Nov. 1972).

[33] D. B. Keele, "Sensitivity of Thiele's Vented Loudspeaker Enclosure Alignments to Parameter Variations," *J. Audio Eng. Soc.*, vol. 21, p. 246 (May 1973).